

Bayesian Markov Renewal Mixed Models for Vocalization Syntax

Yutong Wu

Department of Mechanical Engineering

The University of Texas at Austin

204 E. Dean Keeton Street C2200, Austin, TX 78712-1591, USA

yutong.wu@utexas.edu

Erich D. Jarvis

The Rockefeller University, New York, NY 10065, USA

Howard Hughes Medical Institute, Chevy Chase, MD 20815, USA

ejarvis@rockefeller.edu

Abhra Sarkar

Department of Statistics and Data Sciences

The University of Texas at Austin

2317 Speedway D9800, Austin, TX 78712-1823, USA

abhra.sarkar@utexas.edu

Abstract

Studying the neurological, genetic and evolutionary basis of human vocal communication mechanisms is an important field of neuroscience. In the absence of high-quality data on humans, mouse vocalization experiments in laboratory settings have been proven to be useful in providing valuable insights into mammalian vocal development and evolution, including especially the impact of certain genetic mutations. Data sets from mouse vocalization experiments usually consist of categorical syllable sequences along with continuous inter-syllable interval times for mice of different genotypes vocalizing under various contexts. Few statistical models have considered the inference for both transition probabilities and inter-state intervals. The latter is of particular importance as increased inter-state intervals can be an indication of possible vocal impairment. In this paper, we propose a class of novel Markov renewal mixed models that capture the stochastic dynamics of both state transitions and inter-state interval times. Specifically, we model the transition dynamics and the inter-state intervals using Dirichlet and gamma mixtures, respectively, allowing the mixture probabilities in both cases to vary flexibly with fixed covariate effects as well as random individual-specific effects. We apply our model to analyze the impact of a mutation in the *Foxp2* gene on mouse vocal behavior. We find that genotypes and social contexts significantly affect the inter-state interval times but, compared to previous analyses, the influences of genotype and social context on the syllable transition dynamics are weaker.

Some Key Words: Clustering, Dirichlet mixtures, Gamma mixtures, Markov renewal processes, Mixed effects models, Mouse vocalization experiments

Short Title: Markov Renewal Mixed Models for Vocalization Syntax

Corresponding Author: Abhra Sarkar (abhra.sarkar@utexas.edu)

1 Introduction

This article introduces a novel class of Bayesian mixed models for categorical sequences with continuous inter-state interval times under the influence of multiple exogenous factors. In particular, the values of the exogenous factors remain fixed throughout the sequence and contributes a fixed group effect. Each sequence is also associated with an individual that exhibits a random individual effect. We are interested in the inference of the stochastic dynamics of the sequences, specifically, the transition probabilities of the discrete states and the distribution of the continuous inter-state interval times.

Our research is motivated by the need for sophisticated statistical methods for analyzing mouse vocalization syntax generated in laboratory experiments that are conducted to understand the effects of certain genetic mutations and social contexts on mouse vocal behavior. Such experiments provide clues to the mechanisms underlying human vocalization abilities (Jarvis, 2019). Spoken language plays a crucial role in almost every aspect of human life as we use it to share information, communicate ideas, and express emotions. However, our vocal behaviors might be restrained by a wide variety of impairments, some of which are highly inheritable. According to National Institute on Deafness and Other Communication Disorders, approximately 400,000 individuals in the United States suffer from autism (NIH-NIDCD Report, 2020) the risk of which can be largely traced to inherited genes rather than environmental factors (Bai *et al.*, 2019). It is thus important to study the genetic and evolutionary development of human vocal communication to identify and remedy vocal disorders.

Since data on human vocalization disorders are not easily available, neither can humans be studied under experimentally induced impairing conditions, neuroscientists have turned to studying animal vocalization systems to gain insights into human vocal communication processes. Although unlike speech, the mouse vocalization is mostly innate (Arriaga and Jarvis, 2013; Mooney, 2020) and is a particularly attractive model to study for several reasons. Adult mice ‘sing’ ultrasonic vocalizations (USVs) to communicate with each other. Being mammals, they are also physiologically and genetically similar to us humans. The patterns of USVs may be influenced by the mouse genotype or environmental factors such as stimulating social contexts (Chabout *et al.*, 2015). Mouse vocalization data sets thus typically comprise songs sung by mice from different genotypes under various social contexts. Systematic differences in the syllable dynamics across various genotypes and social conditions can provide insights into their roles on vocal abilities and behavior (Chabout *et al.*, 2016).

Statistical methods for analyzing the syllable dynamics have previously been developed by Holy and Guo (2005); Chabout *et al.* (2015, 2016). Sarkar *et al.* (2018) developed a flexible Bayesian mixed effects Markov model for vocalization syntax incorporating exogenous influences of covariates as well as random heterogeneity of the

sampled mice. While these methods looked in detail into the systematic differences in the syllable dynamics, they did not properly analyze the inter-syllable intervals (ISIs) which can be an additional important indicator of vocal deficits as impaired mice will tend to remain more silent with longer ISIs. To accommodate this effect, the aforementioned methods defined large ISIs as special ‘silent’ syllables and then treated the songs as Markov sequences with this appended vocabulary. This practice, however, largely ignores the differences in the distributions of the ISIs from different mice under various combinations of the covariate values and may miss out important evidence that can be deduced by properly modeling the ISIs.

Here we develop an approach to address these concerns by appropriately analyzing the syllable transition dynamics using the mixed Markov model of Sarkar *et al.* (2018) while also separately modeling the distributions of the ISIs using a novel flexible mixed model of gamma mixtures, thereby providing inference for both syllable transitions dynamics and their ISIs. The method accommodates fixed covariate effects as well as random individual effects in both the syllable transition dynamics and the ISI distributions. A hierarchical cluster inducing mechanism for the levels of the covariates allows straightforward, formal tests of their significance. We design an efficient Markov chain Monte Carlo sampler for fitting our model. We demonstrate the performance of our model by analyzing a data set where the mice are either wild-type or carry a mutation on the Foxp2 gene implicated in causing vocal impairment in humans. Previous analyses of this data set by Chabout *et al.* (2015, 2016); Sarkar *et al.* (2018), with large ISIs treated as an artificial syllable, have shown significant differences in the syllable dynamics between different genotypes and social contexts. When reanalyzed using our proposed approach, the results suggest that genotype and context strongly impact the ISIs, but their influences on the syllable transition dynamics are weaker than what previous analyses had inferred.

Our proposed model is a type of Markov renewal process where the state transitions evolve as a Markov chain while the state durations follow a transition density function that depends on the current state. MRPs were originally introduced by Pyke (1961). MRPs and their variations, including semi-Markov models (Levy, 1954; Smith, 1955), have found success in a variety of applications such as in modeling clinical trials (Weiss and Zelen, 1965), sleeping patterns (Yang and Hursch, 1973), HIV disease occurrences (Foucher *et al.*, 2005), etc. Bayesian methods for MRPs have also been developed. Phelan (1990) designed an MRP where the prior consisted of a family of Dirichlet distributions for transition matrices and a Beta family of Lévy processes for state duration times. Muliere *et al.* (2003) and Bulla and Muliere (2007) developed Bayesian nonparametric reinforced MRPs. Bayesian MRPs with Weibull distributed inter-occurrence times have been developed for seismic data in Alvarez (2005); Epifani *et al.* (2014). Our construction is different from classical MRPs in a number of ways. We model a collection of sequences produced by many different sub-

jects under the influence of multiple external covariates, accommodating fixed effects of the covariates as well as random effects of the subjects in our models for both the transition probability matrices and the distribution of the ISIs. We also allow the selection of important covariates for both the state transition dynamics and the ISI distribution via probabilistic partitioning of the covariate levels. These are in contrast to existing methods on classical MRPs where typically only a single sequence is modeled and the distribution of state duration depends only on the current state.

The remainder of this paper is organized as follows. In Section 2, we provide details of the FoXP2 data set and its scientific background, and review some previous statistical methods. In Section 3, we present our novel Bayesian Markov renewal mixed model. In Section 4, we briefly outline our Markov chain Monte Carlo (MCMC) algorithm to sample from the posterior. In Section 5, we illustrate the results of our method applied to the FoXP2 data set. In Section 6, we summarize the results of a simulation study. Section 7 contains a discussion and some concluding remarks.

2 Data Set and Preliminaries

The FoXP2 data set that we analyze here collects the songs produced by mice of wild-type (W) and mice that have a mutation on the FoXP2 gene (F), a transcription factor that regulates other genes (Chabout *et al.*, 2016). The FoXP2 (foxhead-box P2) gene for mice is found in similar forms in humans (Fisher and Scharff, 2009) and the mutation has been implicated to cause speech and language deficits in adults (Lai *et al.*, 2001). Previously, Fujita *et al.* (2008) compared the vocalizations for wild-type, heterozygous FoXP2 and homozygous FoXP2 mice and showed that both heterozygous and homozygous FoXP2 mice have vocal impairment to some extent. Castellucci *et al.* (2016) showed that mice with a FoXP2 mutation vocalize less and produce shorter syllable sequences. Gaub *et al.* (2016) discovered that compared to wild-type, mice with FoXP2 mutations displayed quantitative differences in USVs.

As discussed in the Introduction, other than genotypes, social contexts can also influence mouse vocalization. Chabout *et al.* (2012) showed that the amount of USVs emitted by male mice is positively correlated with the scale of their social interactions. Gaub *et al.* (2016) studied the USVs of adult mice with increasing stimulus intensity including water and female urine. The FoXP2 data set includes three specific social contexts – fresh female urine on a cotton tip placed inside the male’s cage (U), awake and behaving adult female placed inside the cage (L), and one anesthetized female placed on the lid of the cage (A).

The overall properties of the song syllables provides some information. The sequencing rules of the syllables, call syntax, provides additional information about song complexity. Research has thus also been conducted on the vocabulary and structure of the songs, referred to as ‘syntax’ (Holy and Guo, 2005; Moles *et al.*, 2007; Scat-

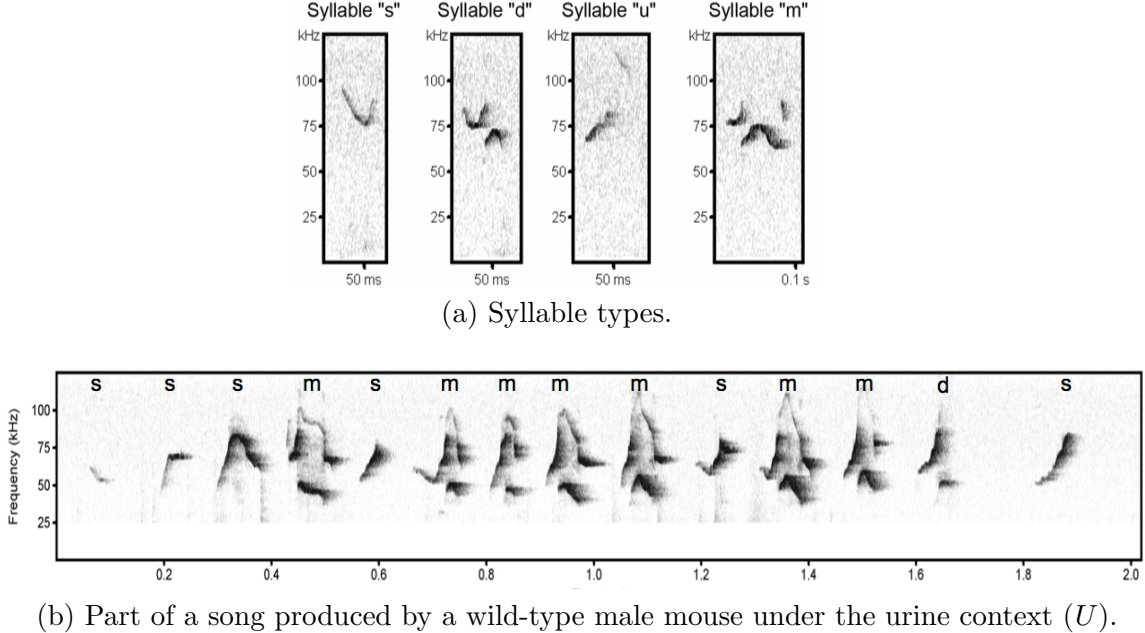


Figure 1: Spectral diagrams of mouse vocalizations, reproduced from Chabout *et al.*, 2016 with permission.

toni *et al.*, 2011; Musolf *et al.*, 2015; Gaub *et al.*, 2016). Adopting the vocabulary in Chabout *et al.* (2012, 2015, 2016), the mouse vocalization syllables can be grouped into four categories based on their spectral features (Figure 1a) as:

- *s*: simple syllables without any pitch jumps;
- *u*: complex syllables with a single upward pitch jump;
- *d*: complex syllables with a single downward pitch jump;
- *m*: more complex syllables with a series of multiple pitch jumps.

Songs are made of a sequential arrangements of these syllables (Figure 1b) with ISIs varying mostly between 0 and 250 milliseconds (Table 1, Figure 2).

Table 2 shows the dynamics of syllable transitions for two different mice under two different contexts from the Foxp2 data set. Since the complexity of the four syllables vary, it is expected that mice with vocal impairments will produce songs with fewer transitions to difficult syllables such as *m*. It is also expected that mice with vocal impairments will tend to remain more silent with longer ISIs. Table 3 shows us the average ISI for mice with different genotypes and under various social contexts, and Figure 2 provides the histograms of ISIs given a genotype or a preceding syllable. Indeed, we see that mice with the Foxp2 mutation are likely to have longer ISI than that of wild-types, especially when the preceding syllable is *m* or *u* for which the averaged ISI is increased by more than 50% (Table 3 and Figure 2a).

Mouse ID	Genotype	Syllable	ISI (in seconds)
1	F	s	0.082
1	F	s	0.017
1	F	m	0.114
\vdots	\vdots	\vdots	\vdots
2	W	s	1.546
2	W	d	0.712
2	W	s	0.549

Table 1: Part of the data set associated with the anesthetized female context (A).

Mouse 1, Foxp2, Context A						Mouse 2, Wildtype, Context L					
	d	m	s	u	Total		d	m	s	u	Total
d	27	17	42	5	91	d	49	47	190	10	296
m	15	10	33	1	59	m	56	76	202	25	359
s	44	29	588	27	688	s	179	216	2224	81	2700
u	5	3	25	2	35	u	12	20	84	8	124

Table 2: Number of transitions from syllables in the left column to syllables in the top row for a Foxp2 mouse and a wild-type mouse singing under contexts A (left) and L (right), respectively.

The development of sophisticated statistical methods for mouse vocalization syntax started with Holy and Guo (2005) who analyzed the songs using a Markov model. Chabout *et al.* (2015, 2016) developed statistical tests for assessing global and local syntax differences across genotypes and social contexts. Sarkar *et al.* (2018) developed a mixed Markov model for the transitions of four syllables and an extra artificial syllable for large ISIs. In the latter three works, each ISI of length greater than 250 milliseconds (ms) was treated as a silent state (' x '). Inference was then performed treating the resulting sequences as Markov chains with five states $\{d, m, s, u, x\}$. Though this was done to achieve significance analytical convenience, the resulting stochastic dynamics also got dominated by transitions to x . However, the distribution of the ISIs varied greatly between different experimental conditions and subjects (Figure 2). Ignoring the ISIs with lengths shorter than 250 ms, as well as treating longer ISIs as blocks of silent syllables, resulted in loss of important information in addition to diluting the transition dynamics among the original syllables. In order to obtain a more accurate inference of the data set, it is important to treat the ISIs differently from the four original syllables and model them properly as a continuous variable.

Our proposed approach addresses these concerns. We model the ISIs separately instead of treating it ad-hocly as the 'silence' syllable. In this way, the ISIs can be used as evidence for vocal impairment aside from the transitions of the four syllables. Moreover, we allow both the transition probabilities and the mixture probabilities for

	W	F
d	0.283	0.433
m	0.168	0.359
s	0.417	0.631
u	0.230	0.547

	U	L	A
d	0.651	0.272	0.281
m	0.373	0.215	0.259
s	0.937	0.339	0.676
u	0.874	0.223	0.613

Table 3: Averaged ISI lengths (in seconds) for mice associated with different genotypes (left) and under different social contexts (right).

the ISIs to be governed by a convex combination of population level fixed effects and individual level random effects.

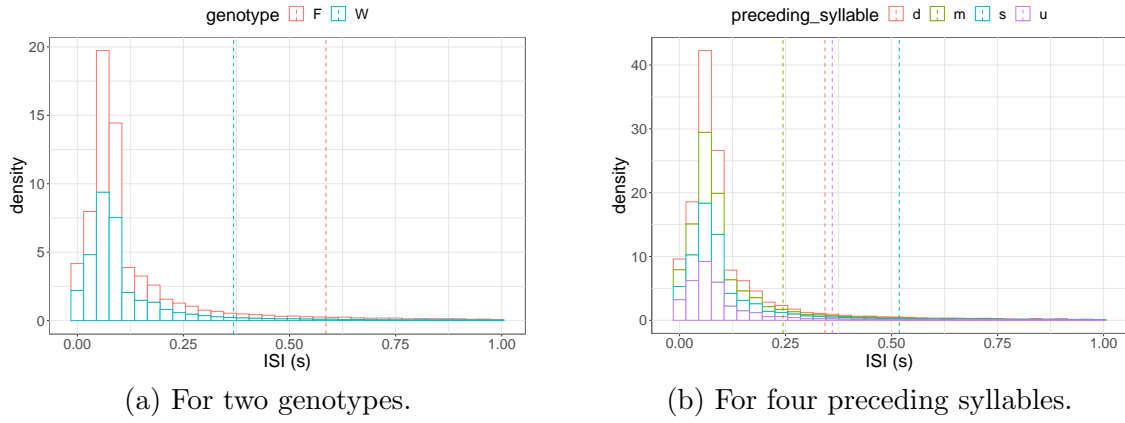


Figure 2: Histogram of ISI grouped by genotypes (left) and preceding syllables (right). Both histograms have long tails. The x-axis is cut off at 1 second for better visualization. The actual range of ISI is from 0.01 seconds to 258.8 seconds.

3 Markov Renewal Mixed Models

In this section, we detail our model for mouse vocalization syntax. Consider a sequence s of T_s syllables. $y_{s,t}$ denotes the syllable at time t for sequence s , and is one of $\mathcal{Y} = \{d, m, s, u\} = \{1, 2, 3, 4\}$. The collection of syllables is denoted by $\{y_{s,t}\}_{s=1,t=1}^{s_0, T_s}$ where s_0 is the total number of sequences. Within a sequence s , we have $T_s - 1$ inter-syllable interval (ISI) times, denoted by $\{\tau_{s,t}\}_{s=1,t=1}^{s_0, T_s - 1}$, where $\tau_{s,t}$ represents the interval time between the t^{th} and $(t+1)^{th}$ syllable for sequence s . Each sequence s is generated under two exogenous factors – genotype $x_{s,1} \in \mathcal{X}_1 = \{F, W\} = \{1, 2\}$, and social context $x_{s,2} \in \mathcal{X}_2 = \{U, L, A\} = \{1, 2, 3\}$, as described in Section 2. With some abuse, we use the same notation to denote the variables as well as their specific values, greatly simplifying the exposition. Table 4 provides a complete list of variables used in our model detailed below.

\mathcal{X}_1	Set of genotypes, $\{F, W\}$
\mathcal{X}_2	Set of social contexts, $\{U, L, A\}$
\mathcal{Y}	Set of four sound syllables, $\{d, m, s, u\}$
$y_{s,t}$	Sound syllable at time t for sequence s , $y_{s,t} \in \mathcal{Y}$
$\tau_{s,t}$	ISI between t^{th} and $(t+1)^{th}$ syllable of sequence s
$x_{s,1}$	Covariate 1, genotype, $x_{s,1} \in \mathcal{X}_1$
$x_{s,2}$	Covariate 2, social context, $x_{s,2} \in \mathcal{X}_2$
$y_{s,t-1}$	Covariate 3, preceding syllable, $y_{s,t-1} \in \mathcal{Y}$

Notations for the Transition Dynamics of the Syllables

$z_{trans,j,x_{s,j}}$	Cluster label of $x_{s,j}$
$\mathcal{C}_{trans}^{(j)}$	Partition of \mathcal{X}_j
$k_{trans,j}$	Number of clusters of partition $\mathcal{C}_{trans}^{(j)}$
$\boldsymbol{\lambda}_{trans,h_1,h_2}$	Transition probability vector for cluster h_1 and h_2
$\boldsymbol{\lambda}_{trans}^{(i)}$	Transition probability vector for mouse i
$\boldsymbol{\lambda}_{trans,0}$	Prior mean of $\boldsymbol{\lambda}_{trans,h_1,h_2}$ and $\boldsymbol{\lambda}_{trans}^{(i)}$
$\boldsymbol{\pi}_{trans,0}^{(i)}$	State-specific probability of fixed effect of mouse i
$\boldsymbol{\pi}_{trans,1}^{(i)}$	State-specific probability of random effect of mouse i

Notations for the Distributions of the Inter-Syllable Intervals

$z_{isi,s,t}$	Component label of gamma mixtures
$z_{isi,r,x_{s,r}}$	Cluster label of $x_{s,r}$
$z_{isi,r,y_{s,t-1}}$	Cluster label of $y_{s,t-1}$
$\mathcal{C}_{isi}^{(r)}$	Partition of $\mathcal{X}_r/\mathcal{Y}$
$k_{isi,r}$	Number of clusters of partition $\mathcal{C}_{isi}^{(r)}$
$\boldsymbol{\lambda}_{isi,g_1,g_2,g_3}$	Mixture probability vector for cluster g_1, g_2 and g_3
$\boldsymbol{\lambda}_{isi}^{(i)}$	Mixture probability vector for mouse i
$\boldsymbol{\lambda}_{isi,0}$	Prior mean of $\boldsymbol{\lambda}_{isi,h_1,h_2}$ and $\boldsymbol{\lambda}_{isi}^{(i)}$
$\boldsymbol{\pi}_{isi,0}^{(i)}$	Component-specific probability of fixed effect of mouse i
$\boldsymbol{\pi}_{isi,1}^{(i)}$	Component-specific probability of random effect of mouse i

Table 4: Notations used in our Markov renewal mixed model for vocalization syntax.

The following result shows that, when the parameters specifying the transition distributions, say $\boldsymbol{\theta}_{trans}$, and the parameters specifying the ISI distributions, say $\boldsymbol{\theta}_{isi}$, have independent priors, they are also conditionally independent in the posterior, simplifying inference. Specifically,

$$\begin{aligned} p(\boldsymbol{\theta}_{trans}, \boldsymbol{\theta}_{isi} | \mathbf{y}, \boldsymbol{\tau}) &\propto p(\mathbf{y} | \boldsymbol{\theta}_{trans}) p(\boldsymbol{\tau} | \boldsymbol{\theta}_{isi}, \mathbf{y}) p_0(\boldsymbol{\theta}_{trans}) p_0(\boldsymbol{\theta}_{isi}) \\ &\propto p(\boldsymbol{\theta}_{trans} | \mathbf{y}) p(\boldsymbol{\theta}_{isi} | \mathbf{y}, \boldsymbol{\tau}), \end{aligned}$$

where $p_0(\cdot)$ denotes a generic for the priors. In what follows, we thus discuss the models for the syllables and the ISIs separately.

3.1 Model for Syllable Transitions

We use the Bayesian mixed effects Markov model of Sarkar *et al.* (2018) for syllable transitions. We describe the model here to keep this article relatively self-contained.

We begin with specifying the transition dynamics as a mixed Markov model as

$$\Pr(y_{s,t} = y_t \mid i_s = i, x_{s,1} = x_1, x_{s,2} = x_2, y_{s,t-1} = y_{t-1}) = P_{trans,x_1,x_2}^{(i)}(y_t \mid y_{t-1}), \quad (1)$$

$$P_{trans,x_1,x_2}^{(i)}(y_t \mid y_{t-1}) = \pi_{trans,0}^{(i)}(y_{t-1})\lambda_{trans,x_1,x_2}(y_t \mid y_{t-1}) + \pi_{trans,1}^{(i)}(y_{t-1})\lambda_{trans}^{(i)}(y_t \mid y_{t-1}).$$

The mixed effects transition probabilities $P_{trans,x_1,x_2}^{(i)}(y_t \mid y_{t-1})$'s are modeled here as a flexible convex mixture of a baseline fixed effect component $\lambda_{trans,x_1,x_2}(\cdot \mid y_{t-1})$ for the exogenous covariates, namely genotype and context, and a random effect component $\lambda_{trans}^{(i)}(\cdot \mid y_{t-1})$ for the mouse. The weights $\pi_{trans,0}^{(i)}$ and $\pi_{trans,1}^{(i)} = 1 - \pi_{trans,0}^{(i)}$ of the two effects are also allowed to be mouse-specific.

For the fixed effects of each covariate j , we try to further identify its levels that have a similar effect on the song dynamics. This is done by creating a probabilistic partition $\mathcal{C}_{trans}^{(j)} = \{\mathcal{C}_{trans,h_j}^{(j)}\}_{h_j=1}^{k_{trans,j}}$ of its levels. Given partitions $\mathcal{C}^{(1)}$ and $\mathcal{C}^{(2)}$, songs with covariates in the same clusters, say $\mathcal{C}_{h_1}^{(1)}$ and $\mathcal{C}_{h_2}^{(2)}$, then share the same baseline transition probability $\lambda_{h_1,h_2}(\cdot \mid y_{t-1})$. The specification of the probabilistic partition models is facilitated by introducing latent cluster allocation variables $\{z_{trans,j,\ell}\}_{j=1,\ell=1}^{2,d_j}$, with $z_{trans,j,\ell}$ indicating the cluster label for the ℓ^{th} level of the j^{th} covariate. Two levels $\ell_1, \ell_2 \in \mathcal{X}_j = \{1, \dots, d_j\}$ will be clustered together if and only if $z_{trans,j,\ell_1} = z_{trans,j,\ell_2}$. For example, $z_{trans,j=2,\ell=2} = z_{trans,j=2,\ell=3} = 1$ means that songs produced under contexts L ($j = 2, \ell = 2$) and A ($j = 2, \ell = 3$) belong to cluster $\mathcal{C}_{h_2=1}^{(j=2)}$ of $\mathcal{C}^{(j=2)}$, etc. Importantly, when the levels of a covariate j are all clustered together, i.e., $k_{trans,j} = 1$, the transition probabilities do not vary with the levels of covariate j . The covariate j thus has no effect on the transition dynamics when $k_{trans,j} = 1$, allowing us to easily and formally test its significance based on the posterior probability of the event $k_{trans,j} = 1$.

Keeping these conditioning variables implicit, the final transition probability of syllables in a song s produced by a mouse $i_s = i$ with genotype $x_{s,1}$ in cluster h_1 and context $x_{s,2}$ in cluster h_2 is given by

$$P_{trans,h_1,h_2}^{(i)}(\cdot \mid y_{t-1}) = \pi_{trans,0}^{(i)}(y_{t-1})\lambda_{trans,h_1,h_2}(\cdot \mid y_{t-1}) + \pi_{trans,1}^{(i)}(y_{t-1})\lambda_{trans}^{(i)}(\cdot \mid y_{t-1}).$$

We assign conditionally conjugate Dirichlet priors to the fixed effect components

$$\lambda_{trans,h_1,h_2}(\cdot \mid y_{t-1}) \sim \text{Dir}\{\alpha_{trans,0}\lambda_{trans,0}(1 \mid y_{t-1}), \dots, \alpha_{trans,0}\lambda_{trans,0}(4 \mid y_{t-1})\}.$$

For the random effects distribution, for any $y_{t-1} \in \mathcal{Y}$, we let

$$\lambda_{trans}^{(i)}(\cdot \mid y_{t-1}) \sim \text{Dir}\left\{\alpha_{trans}^{(0)}\lambda_{trans,0}(1 \mid y_{t-1}), \dots, \alpha_{trans}^{(0)}\lambda_{trans,0}(4 \mid y_{t-1})\right\},$$

$$\pi_{trans,0}^{(i)}(y_{t-1}) \sim \text{Beta}(a_{trans,0}, a_{trans,1}).$$

Centering both $\boldsymbol{\lambda}_{trans,h_1,h_2}$ and $\boldsymbol{\lambda}_{trans}^{(i)}$ around the same mean vector $\boldsymbol{\lambda}_{trans,0}$ facilitates posterior computation. The random effects $\boldsymbol{\lambda}_{trans}^{(i)}$ and $\boldsymbol{\pi}_{trans,0}^{(i)}$ can be easily integrated out to obtain a closed-form expression for population-level probabilities as

$$\mathbf{P}_{trans,h_1,h_2}(\cdot \mid y_{t-1}) = \pi_{trans,0} \boldsymbol{\lambda}_{trans,h_1,h_2}(\cdot \mid y_{t-1}) + \pi_{trans,1} \boldsymbol{\lambda}_{trans,0}(\cdot \mid y_{t-1}),$$

$$\text{where } \pi_{trans,0} = \frac{a_{trans,0}}{a_{trans,0} + a_{trans,1}}, \quad \pi_{trans,1} = \frac{a_{trans,1}}{a_{trans,0} + a_{trans,1}}.$$

We assume that some states in \mathcal{Y} are naturally preferred regardless of the values of the covariates. To capture this, we let $\boldsymbol{\lambda}_{trans,0}$ center around a global $\boldsymbol{\lambda}_{trans,00}$. Lastly, the hyper-parameters $\alpha_{trans}^{(0)}$ and $\alpha_{trans,0}$ are given gamma hyper-priors.

The complete Bayesian hierarchical model for the transition dynamics can then be summarized as follows.

$$\begin{aligned} (y_{s,t} \mid y_{s,t-1} = y_{t-1}, i_s = i, z_{trans,1,x_{s,1}} = h_1, z_{trans,2,x_{s,2}} = h_2) &\sim \\ \text{Mult} \left\{ P_{trans,h_1,h_2}^{(i)}(1 \mid y_{t-1}), \dots, P_{trans,h_1,h_2}^{(i)}(4 \mid y_{t-1}) \right\}, \quad \text{where} \\ \mathbf{P}_{trans,h_1,h_2}^{(i)}(\cdot \mid y_{t-1}) &= \pi_{trans,0}^{(i)}(y_{t-1}) \boldsymbol{\lambda}_{trans,h_1,h_2}(\cdot \mid y_{t-1}) + \pi_{trans,1}^{(i)}(y_{t-1}) \boldsymbol{\lambda}_{trans}^{(i)}(\cdot \mid y_{t-1}), \\ z_{trans,j,\ell} &\sim \text{Mult} \{ \mu_{trans,j}(1), \dots, \mu_{trans,j}(d_j) \}, \\ \boldsymbol{\mu}_{trans,j} &\sim \text{Dir}(\alpha_{trans,j}, \dots, \alpha_{trans,j}), \\ \boldsymbol{\lambda}_{trans}^{(i)}(\cdot \mid y_{t-1}) &\sim \text{Dir} \left\{ \alpha_{trans}^{(0)} \lambda_{trans,0}(1 \mid y_{t-1}), \dots, \alpha_{trans}^{(0)} \lambda_{trans,0}(4 \mid y_{t-1}) \right\}, \\ \boldsymbol{\lambda}_{trans,h_1,h_2}(\cdot \mid y_{t-1}) &\sim \text{Dir} \{ \alpha_{trans,0} \lambda_{trans,0}(1 \mid y_{t-1}), \dots, \alpha_{trans,0} \lambda_{trans,0}(4 \mid y_{t-1}) \}, \\ \boldsymbol{\lambda}_{trans,0}(\cdot \mid y_{t-1}) &\sim \text{Dir} \{ \alpha_{trans,00} \lambda_{trans,00}(1), \dots, \alpha_{trans,00} \lambda_{trans,00}(4) \}, \\ \pi_{trans,0}^{(i)}(y_{t-1}) &\sim \text{Beta}(a_{trans,0}, a_{trans,1}), \\ a_{trans,0} &\sim \text{Ga}(a_{trans,0}, b_{trans,0}), \quad \alpha_{trans}^{(0)} \sim \text{Ga}(a_{trans}^{(0)}, b_{trans}^{(0)}). \end{aligned} \tag{2}$$

3.2 Model for Inter-Syllable Intervals

For the inter-syllable interval (ISI) times $\{\tau_{s,t}\}_{s=1,t=1}^{s_0, T_s-1}$, we associate each ISI from song s with 3 covariates: two exogenous, namely genotype $x_{s,1} \in \mathcal{X}_1 = \{1, 2\}$ and social context $x_{s,2} \in \mathcal{X}_2 = \{1, 2, 3\}$, and one local, namely the preceding syllable $y_{s,t-1} \in \mathcal{Y} = \{1, 2, 3, 4\}$. Given the values of these covariate levels, we model the log-transformed ISI times $\tilde{\tau}_{s,t} = \log(\tau_{s,t} + 1)$ using mixtures of gamma kernels as

$$\begin{aligned} f(\tilde{\tau}_{s,t} \mid i_s = i, x_{s,1} = x_1, x_{s,2} = x_2, y_{s,t-1} = y_{t-1}) \\ = \sum_{k=1}^K P_{isi}^{(i)}(k \mid x_1, x_2, y_{t-1}) \text{Ga}(\tilde{\tau}_{s,t} \mid \alpha_k, \beta_k), \end{aligned} \tag{3}$$

where $\text{Ga}(\cdot \mid \alpha_k, \beta_k)$ denotes a gamma mixture kernel with shape α_k and rate β_k and K is the total number of mixture components. $P_{isi}^{(i)}(k \mid x_1, x_2, y_{t-1})$'s are mixed effects mixture probabilities that vary with the associated covariate values and are also specific to the subject. Introducing latent variables $\{z_{isi,s,t}\}$ indicating the index

of the mixture component, we can write

$$f(\tilde{\tau}_{s,t} \mid z_{isi,s,t} = k) \sim \text{Ga}(\tilde{\tau}_{s,t} \mid \alpha_k, \beta_k),$$

$$\Pr(z_{isi,s,t} = k \mid i_s = i, x_{s,1} = x_1, x_{s,2} = x_2, y_{s,t-1} = y_{t-1}) = P_{isi}^{(i)}(k \mid x_1, x_2, y_{t-1}). \quad (4)$$

Model (4) is structurally similar to model (2) except that we are now modeling the distribution of a latent categorical variable $z_{isi,s,t}$ as opposed to the observed categorical variable $y_{s,t}$. The number of components K in (3) is thus also unknown and needs to be inferred from the data. Nevertheless, we can use similar strategies to model the mixed effects mixture probabilities $P_{isi}^{(i)}(k \mid x_1, x_2, y_{t-1})$ as

$$\mathbf{P}_{x_1, x_2, y_{t-1}}^{(i)}(\cdot) = \pi_{isi,0}^{(i)}(\cdot) \boldsymbol{\lambda}_{isi,x_1,x_2,y_{t-1}}(\cdot) + \pi_{isi,1}^{(i)}(\cdot) \boldsymbol{\lambda}_{isi}^{(i)}(\cdot),$$

where $\boldsymbol{\lambda}_{isi,x_1,x_2,y_{t-1}}(\cdot)$ is the fixed effect component for the associated covariates, namely genotype, context and the preceding syllable, and $\boldsymbol{\lambda}_{isi}^{(i)}(\cdot)$ is the random effect component for the mouse. The weights $\pi_{isi,0}^{(i)}$ and $\pi_{isi,1}^{(i)} = 1 - \pi_{isi,0}^{(i)}$ of the two effects are also allowed to be mouse-specific, as before.

To assess the significance of each covariate r , we induce a clustering $\mathcal{C}_{isi}^{(r)} = \{\mathcal{C}_{isi,g_r}^{(r)}\}_{g_r=1}^{k_{isi,r}}$ of its levels so that ISIs with associated covariates in the same clusters, say g_1 , g_2 and g_3 , share the same fixed effect mixture probability component $\boldsymbol{\lambda}_{isi,g_1,g_2,g_3}$. This is done via introducing latent cluster allocation variables $\{z_{isi,r,w}\}_{r=1,w=1}^{3,d_r}$, as before, with $z_{isi,r,w}$ indicating the cluster label for the w^{th} level of the r^{th} covariate. Importantly, as in the case of transition probabilities, when the levels of a covariate r are all clustered together, i.e., $k_{isi,r} = 1$, the covariate r has no effect on the ISI distribution, allowing us to easily and formally test its significance based on the posterior probability of the event $k_{isi,r} = 1$.

Keeping these conditioning variables implicit, the ISI mixture probability in a song s produced by a mouse $i_s = i$ with genotype $x_{s,1}$ in cluster g_1 and context $x_{s,2}$ in cluster g_2 and preceding syllable $y_{s,t-1}$ in cluster g_3 is given by

$$\mathbf{P}_{isi,g_1,g_2,g_3}^{(i)}(\cdot) = \pi_{isi,0}^{(i)}(\cdot) \boldsymbol{\lambda}_{isi,g_1,g_2,g_3}(\cdot) + \pi_{isi,1}^{(i)}(\cdot) \boldsymbol{\lambda}_{isi}^{(i)}(\cdot).$$

We assign conditionally conjugate Dirichlet priors to the fixed effect components

$$\boldsymbol{\lambda}_{isi,g_1,g_2,g_3}(\cdot) \sim \text{Dir}\{\alpha_{isi,0} \lambda_{isi,0}(1), \dots, \alpha_{isi,0} \lambda_{isi,0}(K)\}.$$

For the random effects distribution, we let

$$\boldsymbol{\lambda}_{isi}^{(i)}(\cdot) \sim \text{Dir}\left\{\alpha_{isi}^{(0)} \lambda_{isi,0}(1), \dots, \alpha_{isi}^{(0)} \lambda_{isi,0}(K)\right\},$$

$$\pi_{isi,0}^{(i)}(k) \sim \text{Beta}(a_{isi,0}, a_{isi,1}).$$

The random effects $\boldsymbol{\lambda}_{isi}^{(i)}$ and $\pi_{isi,0}^{(i)}$ can be easily integrated out to obtain the closed-form population-level mixture probabilities as

$$P_{g_1, g_2, g_3}(k) = \pi_{isi,0} \lambda_{isi,g_1,g_2,g_3}(k) + \pi_{isi,1} \lambda_{isi,0}(k),$$

$$\text{where } \pi_{isi,0} = \frac{a_{isi,0}}{a_{isi,0} + a_{isi,1}}, \quad \pi_{isi,1} = \frac{a_{isi,1}}{a_{isi,0} + a_{isi,1}}.$$

Finally, we let $\boldsymbol{\lambda}_{isi,0}$ center around a global $\boldsymbol{\lambda}_{isi,00}$ and the hyper-parameters $\alpha_{isi}^{(0)}$ and $\alpha_{isi,0}$ are given gamma hyper-priors.

The complete Bayesian hierarchical model for the ISIs may be summarized as

$$\begin{aligned} (\tilde{\tau}_{s,t} | z_{isi,s,t} = k) &\sim \text{Ga}(\tilde{\tau}_{s,t} | \alpha_k, \beta_k), \\ (z_{isi,s,t} | i_s = i, z_{isi,1,x_{s,1}} = g_1, z_{isi,2,x_{s,2}} = g_2, z_{isi,3,y_{s,t-1}} = g_3) &\sim \\ \text{Mult} \left\{ P_{g_1,g_2,g_3}^{(i)}(1), \dots, P_{g_1,g_2,g_3}^{(i)}(K) \right\}, \quad \text{where} \\ P_{g_1,g_2,g_3}^{(i)}(k) &= \pi_{isi,0}^{(i)}(k) \lambda_{isi,g_1,g_2,g_3}(k) + \pi_{isi,1}^{(i)}(k) \lambda_{isi}^{(i)}(k), \\ \boldsymbol{\lambda}_{isi}^{(i)}(\cdot) &\sim \text{Dir} \left\{ \alpha_{isi}^{(0)} \lambda_{isi,0}(1), \dots, \alpha_{isi}^{(0)} \lambda_{isi,0}(K) \right\}, \quad \alpha_{isi}^{(0)} \sim \text{Ga}(a_{isi}^{(0)}, b_{isi}^{(0)}), \\ \boldsymbol{\lambda}_{isi,g_1,g_2,g_3}^{(i)}(\cdot) &\sim \text{Dir} \left\{ \alpha_{isi,0} \lambda_{isi,0}(1), \dots, \alpha_{isi,0} \lambda_{isi,0}(K) \right\}, \quad \alpha_{isi,0} \sim \text{Ga}(a_{isi,0}, b_{isi,0}), \\ \boldsymbol{\lambda}_{isi,0}^{(i)}(\cdot) &\sim \text{Dir} \left\{ \alpha_{isi,00} \lambda_{isi,00}(1), \dots, \alpha_{isi,00} \lambda_{isi,00}(K) \right\}, \\ \pi_{isi,0}^{(i)}(k) &\sim \text{Beta}(a_{isi,0}, a_{isi,1}), \\ \alpha_k &\sim \text{Ga}(a_{isi,0}, b_{isi,0}), \quad \beta_k \sim \text{Ga}(a_{isi,0}, b_{isi,0}). \end{aligned} \tag{5}$$

Gamma mixtures, in simpler forms, have appeared before in Chen (2000); Wiper *et al.* (2001), etc. The gamma kernel, however, brings in computational challenges which we address briefly in Section 4 below and then in detail again in Section S.3 in the supplementary materials. There also exists some literature on flexible mixture and partition models for conditionally varying densities of continuous random variables in the presence of covariates (MacEachern, 1999; Chung and Dunson, 2009; Müller *et al.*, 2011, etc.). To our knowledge, however, flexible mixed effects mixture models of the type proposed here that accommodate both fixed effects of covariates as well as random heterogeneity of subjects while also allowing simultaneous covariate selection have not appeared in the literature before.

4 Prior Hyper-parameters and Posterior Inference

The choice of prior hyper-parameters, including the choice of the number of mixture components K in the gamma mixture model (3) for which we use predictive model selection criteria, are discussed in Section S.1 in the supplementary materials.

Our posterior inference is based on samples of the model parameters drawn using an MCMC algorithm. The full conditional posterior distributions are mostly obtained in closed-form and hence are easy to sample from. One exception is the sampling of the gamma mixture parameters. The conjugate prior for gamma distribution with unknown shape parameter is known to be analytically intractable (Damsleth, 1975; Miller, 1980), posing difficulty in sampling the parameters α_k 's and β_k 's. We experi-

mented a number of sampling methods and ultimately used the strategy introduced in Miller (2019) which uses a gamma density function to approximate the full conditional for gamma shape parameters. After sampling the shape parameters α_k 's, the rate parameters β_k 's can be easily sampled from their closed-form conjugate gamma full conditionals. As the results of Sections 5 and 6 will illustrate, this method worked well with real data as well as in our simulation experiments, converging quickly, mixing well and providing accurate estimates of the target distributions. Details of the posterior sampling algorithm can be found in Section S.3 in the supplementary materials.

5 Results for the Foxp2 Data Set

In this section, we discuss the results of the proposed Bayesian Markov renewal mixed model fitted to the Foxp2 data set. We present the results for syllable transitions and ISIs separately. In Section 5.1, we analyze the influence of genotypes and social contexts on syllable transitions. In Section 5.2, we analyze the influence of genotypes, social contexts and the preceding syllable on the distribution of the ISIs.

5.1 Results for Syllable Transition

Figure 3 shows the estimated posterior mean of the population-level transition probabilities, $P_{trans,x_1,x_2}(y_t | y_{t-1})$, given genotype x_1 and social context x_2 . We see that regardless of the covariate values, the s syllable is predominantly transitioned to and u is the least likely syllable to transition to across different genotypes and contexts. This is reasonable since the s syllable is presumably the easiest to pronounce and u is the least pronounced syllable across all sequences.

Consider the following hypotheses for the impact of genotype and social context.

- $H_{trans,0,j}$: The population-level transition probabilities $P_{trans,x_1,x_2}(y_t | y_{t-1})$ do not vary based on values of $x_j, j = 1, 2$.
- $H_{trans,1,j}$: The population-level transition probabilities $P_{trans,x_1,x_2}(y_t | y_{t-1})$ vary based on values of $x_j, j = 1, 2$.

By the construction of our model, $H_{trans,1,j}$ is true if and only if $k_{trans,j} > 1$. Figure 4 displays the estimated posterior distribution of $k_{trans,j}$ for genotype $x_{j=1}$ and social context $x_{j=2}$. The estimated posterior probability that $k_{trans,1}$ greater than 1 is $\hat{P}(k_{trans,1} > 1 | \text{data}) \approx 0.56$. In contrast to the findings reported previously in Sarkar *et al.* (2018), the evidence that the mutation on the Foxp2 gene impacts the transition probabilities of the syllables has thus become somewhat weaker. This illustrates that treating ISI as a separate continuous variable results in less distinctions

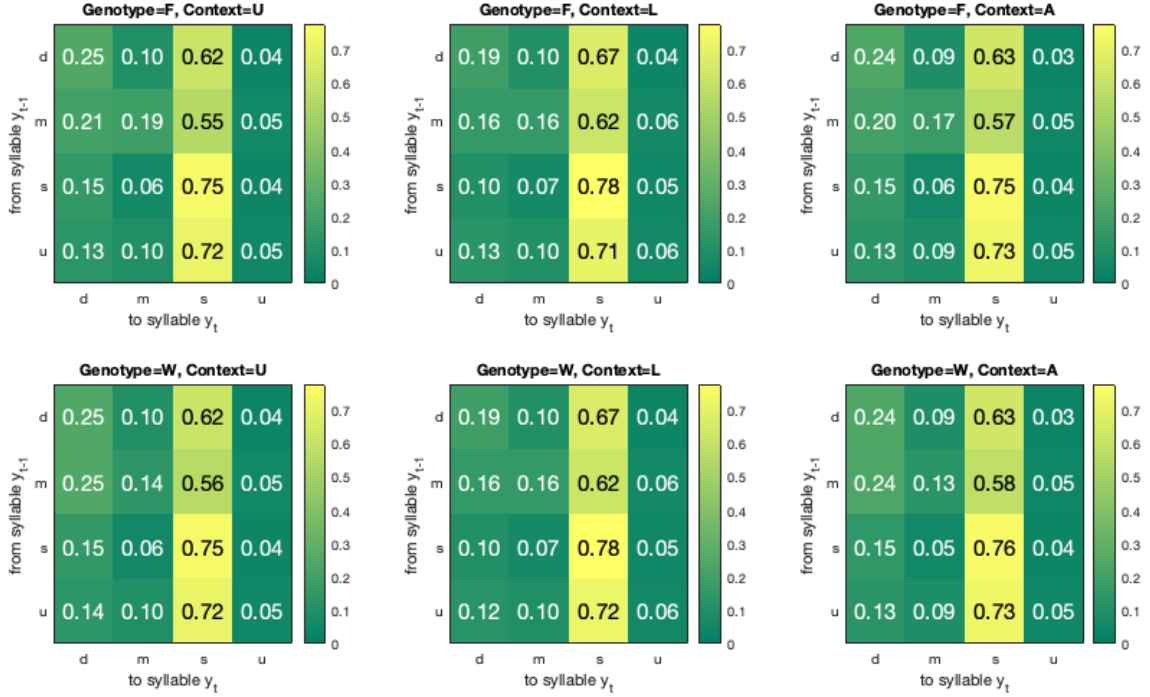


Figure 3: Results for transitions for the Foxy2 data set showing the estimated posterior mean of the transition probabilities $P_{trans,x_1,x_2}(y_t | y_{t-1})$ of syllables $y_t, y_{t-1} \in \mathcal{Y} = \{d, m, s, u\}$ under different combinations of genotype $x_1 \in \{F, W\}$ and social context $x_2 \in \{U, L, A\}$.

between the transition dynamics of the two groups. Conforming to the previous analyses in Sarkar *et al.* (2018), there is, however, very clear evidence of the influence of social context on the transitions probabilities. In Figure 4, we see that the estimated posterior probability $\widehat{P}(k_{trans,2} > 1 | \text{data}) = 1$, with $\widehat{P}(k_{trans,2} = 2 | \text{data}) = 0.58$ and $\widehat{P}(k_{trans,2} = 3 | \text{data}) = 0.42$. Specifically, whenever there were two clusters, the contexts U and A were clustered together. In Figure 3, we see that there is strong evidence that contexts U and A have similar impact across genotypes. Compared to U and A , the L context has smaller transition probabilities for transitions types $d \rightarrow d$ and $m \rightarrow d$ across the two genotypes. The decrease in the transition probabilities of $d \rightarrow d$ and $m \rightarrow d$ seems to be explained by the increase in the probabilities of $d \rightarrow s$ and $m \rightarrow s$, suggesting that the mice vocalized short and simple symbols more often under the L context.

5.2 Results for Inter-Syllable Intervals

We first transform the observed ISIs to $\tilde{\tau}_{s,t} = \log(1 + \tau_{s,t})$. The original $\tau_{s,t}$'s have a wide range with a minimum of 0.01 and a maximum of 258.8 seconds. This pre-processing step helps shorten the range of the data and produce better visualizations

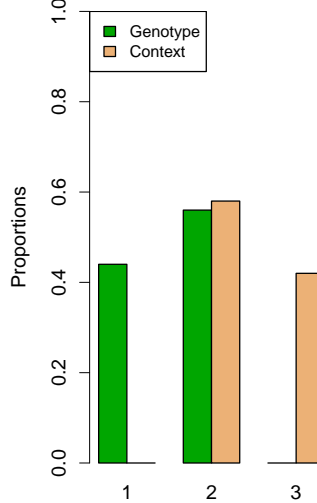
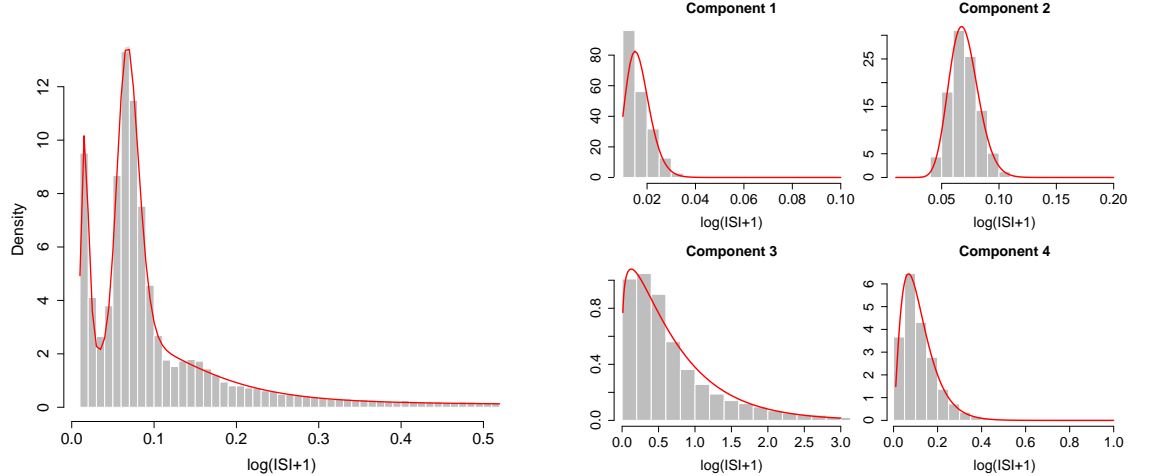


Figure 4: Results for the Foxp2 data set showing the proportions of the number of clusters $k_{trans,j}$ for each covariate j among thinned samples after burn-ins for syllable transitions. The x-axis represents the number of clusters. The green/orange bars represent the posterior distribution of $P(k_{trans,j})$ for genotype $x_{j=1} \in \{F, W\}$ and social context $x_{j=2} \in \{U, L, A\}$, respectively.

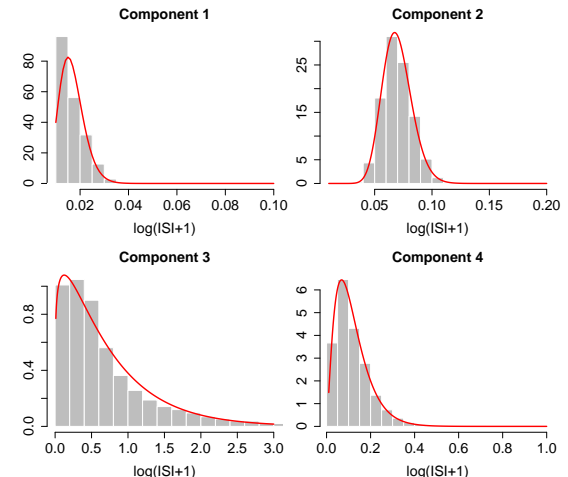
for results. We add 1 to the original $\tau_{s,t}$'s before taking the log to avoid negative $\tilde{\tau}_{s,t}$'s.

The left panel of Figure 5 shows the histogram of the transformed ISIs along with the posterior mean (red curve) averaged from samples after burn-ins and thinning. We see that our proposed model fits the ISI data very well, whose two peaks are captured by the mixture gamma distribution. The right panels of Figure 5 display the histogram for each mixture component along with the corresponding gamma densities with shape and rate parameters taken from the last iteration of the MCMC sampler. It is clear that components 1, 2 and 4 represent the two peaks we see in the left panel of Figure 5 whereas components 3 and 4 assign more probability mass to larger values of the transformed ISIs. The shape and rate parameters for the gamma distribution of each component are presented in the leftmost panel of Figure 5c. The shape and rate parameters for components 1 and 2 are much larger than those of components 3 and 4, capturing the concentration of the small values of the transformed ISIs.

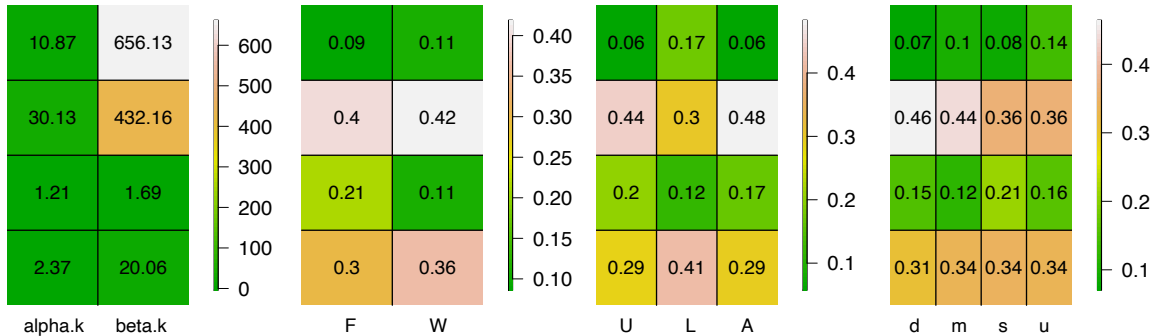
Figure 5c also displays the mixture probabilities taken from the last MCMC iteration for each covariate: genotype (F and W), social contexts (U , L , and A), and preceding syllables (d , m , s and u). We see that mice with the Foxp2 mutation have a smaller mixture probability in the components 1, 2 and 4 compared to wild-types but have a significantly higher probability for component 3 (+0.1). Recall that component 3 has the smallest rate parameter, which indicates a higher probability to have a larger value compared to the other components. A large mixture probability in component 3 indicates a high ISI value. This suggests that the ISI length for mice with the Foxp2 mutation concentrates on larger values than the ISIs of wild-types,



(a) Histogram of the transformed ISIs with the estimated posterior mean (red line) of their marginal gamma mixture density based on MCMC samples after burn-in and thinning.



(b) Histograms of the transformed ISIs for each component of the gamma mixture model along with the component density (red lines) from the last MCMC iteration. The x-axes are adjusted for better visualization.



(c) Mixture parameters and associated mixture probabilities for different covariates. The leftmost panel displays the estimated gamma shape and rate parameters taken from the last iteration of MCMC sampler. Each row represents a component. The next three panels from left to right: mixture probabilities with respect to four components for genotype $x_1 \in \{F, W\}$, social context $x_2 \in \{U, L, A\}$ and preceding syllable $y_{t-1} \in \{d, m, s, u\}$, respectively, for the last MCMC iteration.

Figure 5: Results for ISIs for the Foxp2 data set.

which supports our hypothesis that mice with such mutation needs a longer ISI before pronouncing a new syllable.

One interesting discovery from Figure 5c is that male mice in the presence of a live female (L context) tend to have shorter ISIs than those under the other two contexts since the mixture probability is high in component 1 but low in component 3 for the L context. This suggests that male mice need a shorter interval between pronouncing two syllables in the presence of a live female. This finding, along with the discovery

that transitions to the simplest syllable s are more frequent under the L context, shows that male mice exhibit different vocalization dynamics when there is an awake female mouse present.

On the rightmost panel of Figure 5c, we see the mixture probabilities associated with each preceding syllable. All four syllables have similar weights for component 1 but syllable s has a much higher weight for component 2, indicating a shorter ISI after producing syllable s . This is reasonable as s is a simple syllable to pronounce. On the other hand, syllables d and m have a higher mixture probability in component 3, suggesting that mice need a longer interval time to pronounce the next syllable after producing d and m , suggesting that these two syllables maybe more difficult to produce.

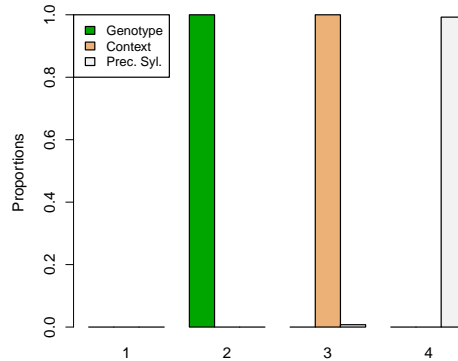


Figure 6: Results for the Foxp2 data set showing the proportions of the number of clusters $k_{isi,r}$ for each covariate r among thinned samples after burn-ins. The x-axis represents the number of clusters. The green/orange/white bars represent the posterior distribution of $P(k_{isi,r})$ for genotype $x_1 \in \{F, W\}$, social context $x_2 \in \{U, L, A\}$ and preceding syllable $y_{t-1} \in \{d, m, s, u\}$, respectively.

We are also interested in testing the significance of the impact each covariate has on the ISIs. In particular, let $H_{isi,0,r}$ be the hypothesis that the distribution of ISI does not vary with the values of the covariate r . Similar to syllable transitions, $H_{isi,0,r}$ is true if and only if $k_{isi,r} = 1$. In Figure 6, we plot the estimated posterior probabilities $\widehat{P}(k_{isi,r} | \text{data})$ for each covariate r . We have $\widehat{P}(k_{isi,r} = d_r | \text{data}) = 1$ for $r = 1, 2$, implying strong evidence of the influence of genotypes and social contexts on the distribution of the ISIs. For preceding syllables, $\widehat{P}(k_{isi,r=3} = d_3 | \text{data}) > 0.99$. Therefore, all three covariates, genotypes, social contexts and preceding syllables, are highly significant for the distribution of ISIs.

6 Simulation Studies

We designed simulation experiments to evaluate the performance of the proposed MRP in assessing mouse vocalization dynamics. We are not aware of any other model

for vocalization syntax that can be directly compared with ours. We thus focus here on evaluating the performance of our proposed method in recovering an underlying ‘truth’. Also, since the mixed Markov model was evaluated in detail in Sarkar *et al.* (2018), we focus mainly on evaluating the model for the ISIs here. In designing our simulation truths, we try to closely mimic the FoXP2 data set, including sampling the syllables $\{d, m, s, u\}$ and the ISIs using the transition probabilities and the gamma mixtures estimated in Section 5 as the corresponding truths. We consider 18 mice, 10 with the FoXP2 mutation and 8 wild-types, that sing under three social contexts, $\{U, L, A\}$. The first syllable for each sequence is copied from the FoXP2 data set and the rest are sampled using the transition probabilities presented in Figure 3. Given genotype, context and the preceding syllable, ISI is then sampled using the gamma mixture shown in Figure 5c. We set the number of mixture components to be $K = 4$ and analyze the following scenarios.

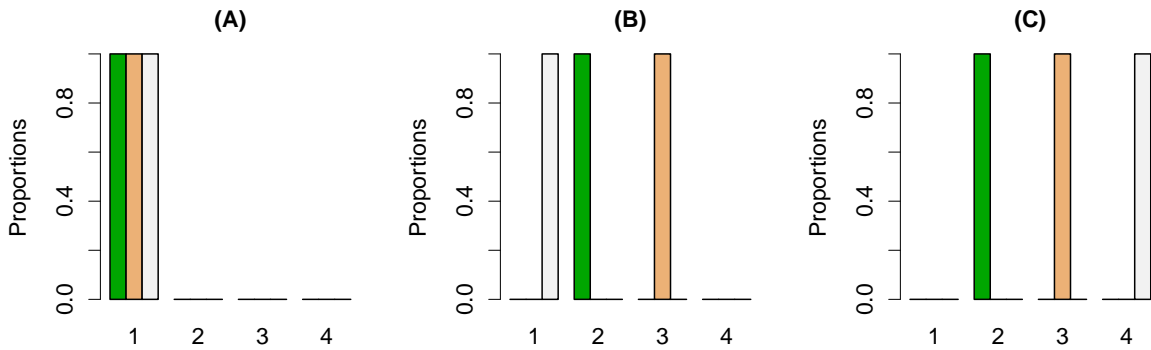


Figure 7: Results of the simulation studies showing the percentages of the number of clusters $k_{isi,r}$ for each covariate r among thinned samples after burn-ins for every study. The x-axis represents the number of clusters. The green/orange/white bar represents the estimated posterior distribution of $P(k_{isi,r})$ for genotype $x_1 \in \{F, W\}$, social context $x_2 \in \{U, L, A\}$ and preceding syllable $y_{t-1} \in \{d, m, s, u\}$, respectively. The results agree with the scenario settings for each simulation study.

- (A) $\lambda_{isi,x_1,x_2,y_{t-1}} = \hat{\lambda}_{isi,1,1,1}$ for $x_1 = 1, 2$, $x_2 = 1, 2, 3$ and $y_{t-1} = 1, 2, 3, 4$. ISI does not vary with genotype, context or the preceding syllable ($k_{isi,1,0} = 1$, $k_{isi,2,0} = 1$, $k_{isi,3,0} = 1$).
- (B) $\lambda_{isi,x_1,x_2,y_{t-1}} = \hat{\lambda}_{isi,x_1,x_2,1}$ for $x_1 = 1, 2$, $x_2 = 1, 2, 3$ and $y_{t-1} = 1, 2, 3, 4$. ISI varies with genotype and context but does not vary with the preceding syllable ($k_{isi,1,0} = 2$, $k_{isi,2,0} = 3$, $k_{isi,3,0} = 1$).
- (C) $\lambda_{isi,x_1,x_2,y_{t-1}} = \hat{\lambda}_{isi,x_1,x_2,y_{t-1}}$ for $x_1 = 1, 2$, $x_2 = 1, 2, 3$ and $y_{t-1} = 1, 2, 3, 4$. ISI varies with genotype, context and the preceding syllable ($k_{isi,1,0} = 2$, $k_{isi,2,0} = 3$, $k_{isi,3,0} = 4$).

Figure 7 displays the estimated posterior probability $\hat{P}(k_{isi,r} | \text{data})$ for each covariate r . We see that $\hat{P}(k_{isi,r} = k_{isi,r0} | \text{data}) \approx 1$ for every scenario, showing great performance of our method in testing the relevant hypotheses. Study (C) is the closest to the Foxp2 data set where all of the covariates are significant for the ISIs, and we now compare the results from study (C) to those of the Foxp2 data set. We first look at the estimated posterior mean for transition probabilities under every combination of genotype and social context, presented in Figure 8. For every transition type, given genotype and social context, the estimated transition probability is very close to that of the Foxp2 data set (Figure 3). Next, we turn to the results for ISIs. Figure 9 (left panel) displays the histogram of the simulated data superimposed over the estimated posterior mean ISI distribution. The shape of the synthesized data looks close to the real data set (Figure 5) and the estimated posterior density fits the data well. The histogram of ISIs for each component of the mixture gamma is presented in Figure 9 (right panels) along with their estimates from the last MCMC iteration. We observe that due to label switching, the original components 1, 2, 3, 4 now correspond to components 4, 3, 2, 1, respectively. The estimated values of gamma mixture parameters are presented in the leftmost panel of Figure 9c. Accounting for label switching, the shape and the rate parameters are both similar to the corresponding estimated values for the Foxp2 data set (Figure 5c). Similarly, the mixture probabilities for each covariate as shown in the three right panels of Figure 9c also agree with the corresponding simulation truths. The performance of our method in all of the different simulation scenarios, including scenario (C) where the simulation design closely matched the real data results in Section 5, show that our model is capable of assessing the mouse vocalization dynamics under a wide range of realistic scenarios.

7 Discussion

This paper introduced a new class of Bayesian Markov renewal mixed effects models that allows inference of both state transition probabilities and continuous inter-state interval times. On the statistical side, our main novel contribution is a mixed effects gamma mixture model for the inter-state intervals. The mixture probabilities build on carefully constructed convex combinations of a fixed effect component for the associated covariates and a random effect component for the associated individual, resulting in a highly flexible and computationally tractable model. At the same time, covariate values that induce similar effects on the response are probabilistically clustered together and significant covariates are identified.

We used the model to reanalyze the Foxp2 data set which comprises a collection of songs sung by adult male mice with or without a Foxp2 mutation under various social contexts. In contrast to previous analyses, we found weaker evidence that the transition dynamics of the syllables within the songs vary with genotype and social

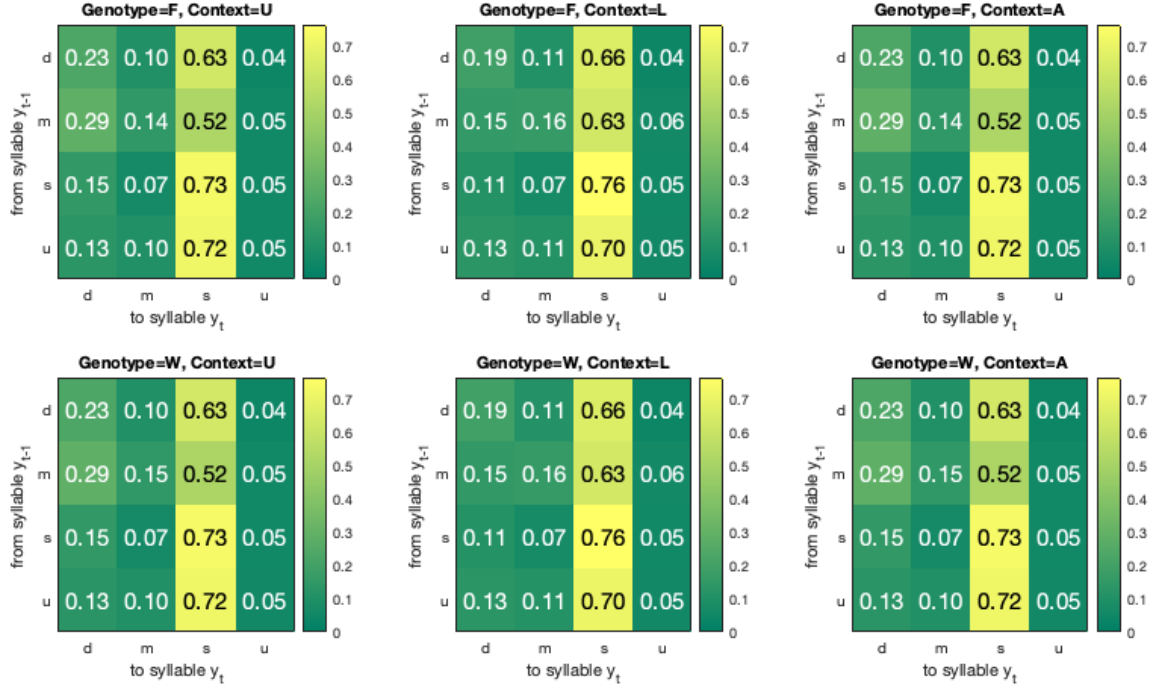


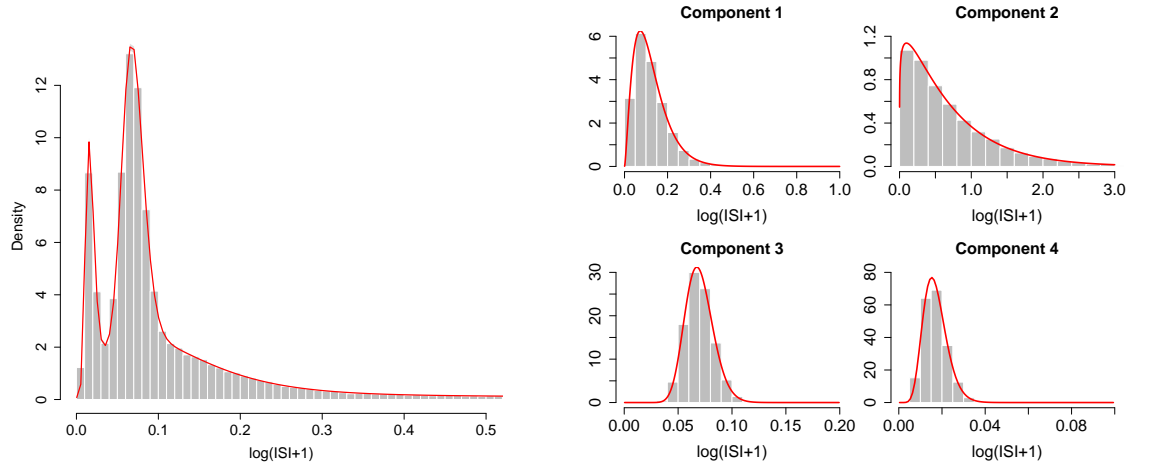
Figure 8: Results for transitions for simulation design (C) showing the estimated posterior mean of the transition probabilities $P_{trans,x_1,x_2}(y_t | y_{t-1})$ of syllables $y_t, y_{t-1} \in \mathcal{Y} = \{d, m, s, u\}$ under different combinations of genotype $x_1 \in \{F, W\}$ and social context $x_2 \in \{U, L, A\}$.

context. On the other hand, there is significant evidence that all three covariates, namely genotypes, social contexts, and preceding syllables, influence the lengths of the ISIs. On the application side, the important scientific implication is that the vocal impairment of the *Foxp2* mice is manifested in their having longer ISIs than wild-types, not just in the syllable transition dynamics as previous analyses suggested.

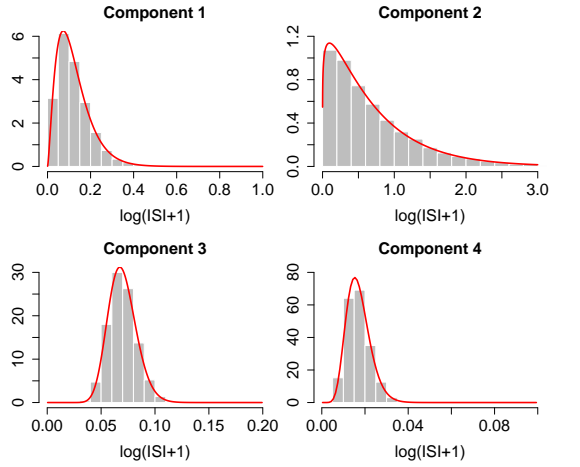
The proposed model is quite genetic in nature and hence can be used to analyze other data sets comprising categorical sequences and associated continuous inter-state interval times, both of which may potentially be influenced by various exogenous factors as well as subject-specific heterogeneity. Our model also points to possible directions of research in Markov renewal models that consider different aspects of state transitions (transition probabilities, inter-state intervals, state durations, etc.) and help make novel discoveries in important practical applications.

Supplementary Materials

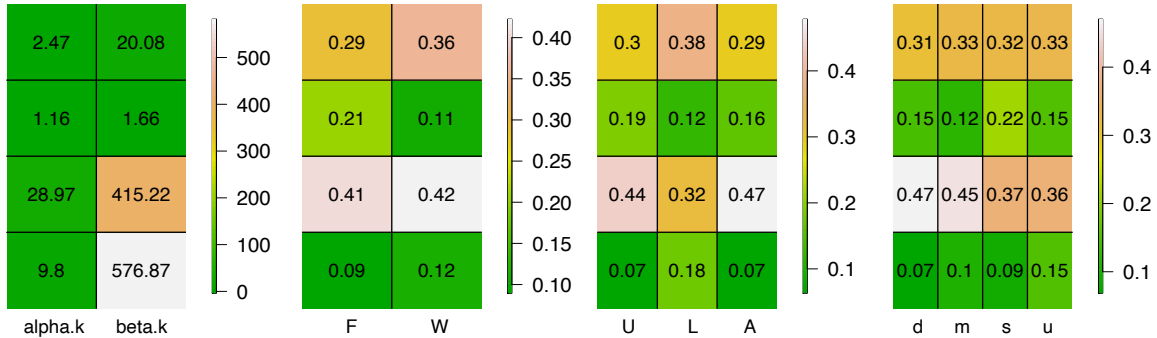
The supplementary materials discuss the choice of the prior hyper-parameters and details of the MCMC sampler. Our implementation is in R and the instructions to use the codes are included in a ‘readme’ file in the supplemental materials.



(a) Histogram of the transformed ISIs with the estimated posterior mean (red line) of their marginal gamma mixture density based on MCMC samples after burn-in and thinning.



(b) Histograms of the transformed ISIs for each component of the gamma mixture model along with the component density (red lines) from the last MCMC iteration. The x-axes are adjusted for better visualization.



(c) Mixture parameters and associated mixture probabilities for different covariates. The leftmost panel displays the estimated gamma shape and rate parameters taken from the last iteration of MCMC sampler. Each row represents a component. The next three panels from left to right: mixture probabilities with respect to four components for genotype $x_1 \in \{F, W\}$, social context $x_2 \in \{U, L, A\}$ and preceding syllable $y_{t-1} \in \{d, m, s, u\}$, respectively, for the last MCMC iteration.

Figure 9: Results for ISIs for simulation design (C).

References

Alvarez, E. E. (2005). Estimation in stationary Markov renewal processes, with application to earthquake forecasting in Turkey. *Methodology and Computing in Applied Probability*, **7**, 119–130.

Arriaga, G. and Jarvis, E. D. (2013). Mouse vocal communication system: Are ultrasounds learned or innate? *Brain and Language*, **124**, 96–116.

Bai, D., Yip, B. H. K., Windham, G. C., Sourander, A., Francis, R., Yoffe, R.,

Glasson, E., Mahjani, B., Suominen, A., Leonard, H., *et al.* (2019). Association of genetic and environmental factors with autism in a 5-country cohort. *JAMA Psychiatry*, **76**, 1035–1043.

Bulla, P. and Muliere, P. (2007). Bayesian nonparametric estimation for reinforced Markov renewal processes. *Statistical Inference for Stochastic Processes*, **10**, 283–303.

Castellucci, G. A., McGinley, M. J., and McCormick, D. A. (2016). Knockout of Foxp2 disrupts vocal development in mice. *Nature Scientific Reports*, **6**. doi: 10.1038/srep23305.

Chabout, J., Serreau, P., Ey, E., Bellier, L., Aubin, T., Bourgeron, T., and Granon, S. (2012). Adult male mice emit context-specific ultrasonic vocalizations that are modulated by prior isolation or group rearing environment. *PLoS ONE*, **7**:e29401. doi: 10.1371/journal.pone.0046610.

Chabout, J., Sarkar, A., Dunson, D. B., and Jarvis, E. D. (2015). Male song syntax depends on contexts and influences female preferences in mice. *Frontiers in Behavioral Neuroscience*, **9**, 1–19.

Chabout, J., Sarkar, A., Patel, S., Raiden, T., Dunson, D. B., Fisher, S. E., and Jarvis, E. D. (2016). A Foxp2 mutation implicated in human speech deficits alters sequencing of ultrasonic vocalizations in adult male mice. *Frontiers in Behavioral Neuroscience*, **10**, 1–18.

Chen, S. X. (2000). Probability density function estimation using gamma kernels. *Annals of the Institute of Statistical Mathematics*, **52**, 471–480.

Chung, Y. and Dunson, D. B. (2009). Nonparametric Bayes conditional distribution modeling with variable selection. *Journal of the American Statistical Association*, **104**, 1646–1660.

Damsleth, E. (1975). Conjugate classes for Gamma distributions. *Scandinavian Journal of Statistics*, **2**, 80–84.

Epifani, I., Ladelli, L., and Pievatolo, A. (2014). Bayesian estimation for a parametric Markov renewal model applied to seismic data. *Electronic Journal of Statistics*, **8**, 2264–2295.

Fisher, S. E. and Scharff, C. (2009). Foxp2 as a molecular window into speech and language. *Trends in Genetics*, **25**, 166–177.

Foucher, Y., Mathieu, E., Saint-Pierre, P., Durand, J.-F., and Daurès, J.-P. (2005). A semi-Markov model based on generalized Weibull distribution with an illustration for HIV disease. *Biometrical Journal: Journal of Mathematical Methods in Biosciences*, **47**, 825–833.

Fujita, E., Tanabe, Y., Shiota, A., Ueda, M., Suwa, K., Momoi, M. Y., and Momoi, T. (2008). Ultrasonic vocalization impairment of Foxp2 (R552H) knockin mice related to speech-language disorder and abnormality of Purkinje cells. *Proceedings of the National Academy of Sciences*, **105**, 3117–3122.

Gaub, S., Fisher, S. E., and Ehret, G. (2016). Ultrasonic vocalizations of adult male Foxp2 mutant mice: behavioral contexts of arousal and emotion. *Genes, Brain and Behavior*, **15**, 243–259.

Holy, T. E. and Guo, Z. (2005). Ultrasonic songs of male mice. *PLoS Biology*, **3**, 2177–2186.

Jarvis, E. D. (2019). Evolution of vocal learning and spoken language. *Science*, **366**, 50–54.

Lai, C. S., Fisher, S. E., Hurst, J. A., Vargha-Khadem, F., and Monaco, A. P. (2001). A forkhead-domain gene is mutated in a severe speech and language disorder. *Nature*, **413**, 519–523.

Levy, P. (1954). Processus semi-Markoviens. In *Proceedings of International Congress of Mathematics*.

MacEachern, S. N. (1999). Dependent nonparametric processes. In *ASA proceedings of the section on Bayesian statistical science*, pages 50–55. Alexandria, Virginia: American Statistical Association.

Miller, J. W. (2019). Fast and accurate approximation of the full conditional for Gamma shape parameters. *Journal of Computational and Graphical Statistics*, **28**, 476–480.

Miller, R. B. (1980). Bayesian analysis of the two-parameter Gamma distribution. *Technometrics*, **22**, 65–69.

Moles, A., Costantini, F., Garbugino, L., Zanettini, C., and DÁmato, F. R. (2007). Ultrasonic vocalizations emitted during dyadic interactions in female mice: A possible index of sociability? *Behavioural Brain Research*, **182**, 223—230.

Mooney, R. (2020). The neurobiology of innate and learned vocalizations in rodents and songbirds. *Current opinion in neurobiology*, **64**, 24–31.

Muliere, P., Secchi, P., and Walker, S. G. (2003). Reinforced random processes in continuous time. *Stochastic Processes and their Applications*, **104**, 117–130.

Müller, P., Quintana, F., and Rosner, G. L. (2011). A product partition model with regression on covariates. *Journal of Computational and Graphical Statistics*, **20**, 260–278.

Musolf, K., Meindl, S., Larsen, A. L., Kalcounis-Rueppell, M. C., and J., P. D. (2015). Ultrasonic vocalizations of male mice differ among species and females show assortative preferences for male calls. *PLoS ONE*, **10:e0134123**. doi:10.1371/journal.pone.0134123.

NIH-NIDCD Report (2020). Statistics on voice, speech, and language. <https://www.nidcd.nih.gov/health/statistics/statistics-voice-speech-and-language>.

Phelan, M. J. (1990). Bayes estimation from a Markov renewal process. *The Annals of Statistics*, **18**, 603–616.

Pyke, R. (1961). Markov renewal processes: definitions and preliminary properties. *The Annals of Mathematical Statistics*, **32**, 1231–1242.

Sarkar, A., Chabout, J., Macopson, J. J., Jarvis, E. D., and Dunson, D. B. (2018). Bayesian semiparametric mixed effects Markov models with application to vocalization syntax. *Journal of the American Statistical Association*, **113**, 1515–1527.

Scattoni, M. L., Ricceri, L., and Crawley, J. N. (2011). Unusual repertoire of vocalizations in adult BTBR T+tf/J mice during three types of social encounters. *Genes, Brain and Behavior*, **10**, 44–56.

Smith, W. L. (1955). Regenerative stochastic processes. *Proceedings of the Royal Society of London. Series A. Mathematical and Physical Sciences*, **232**, 6–31.

Weiss, G. H. and Zelen, M. (1965). A semi-Markov model for clinical trials. *Journal of Applied Probability*, **2**, 269–285.

Wiper, M., Insua, D. R., and Ruggeri, F. (2001). Mixtures of gamma distributions with applications. *Journal of computational and graphical statistics*, **10**, 440–454.

Yang, M. C. and Hursch, C. J. (1973). The use of a semi-Markov model for describing sleep patterns. *Biometrics*, **29**, 667–676.

Supplementary Materials for

Bayesian Markov Renewal Mixed Models for Vocalization Syntax

Yutong Wu

Department of Mechanical Engineering

The University of Texas at Austin

204 E. Dean Keeton Street C2200, Austin, TX 78712-1591, USA

yutong.wu@utexas.edu

Erich D. Jarvis

The Rockefeller University, New York, NY 10065, USA

Howard Hughes Medical Institute, Chevy Chase, MD 20815, USA

ejarvis@rockefeller.edu

Abhra Sarkar

Department of Statistics and Data Sciences

The University of Texas at Austin

2317 Speedway D9800, Austin, TX 78712-1823, USA

abhra.sarkar@utexas.edu

The supplementary materials provide details of the choice of the hyper-parameters in Section S.1, MCMC initialization in Section S.2, and a step-by-step posterior computation in Section S.3. The R code and the corresponding instructions are provided in Supplemental Materials for interested readers.

S.1 Choice of Hyper-Parameters

S.1.1 Hyper-Parameters for Syllable Transitions

For the inference of the transition of syllables, we set $\alpha_{trans,00} = 1$ and $\lambda_{trans,00}(y_t) = \sum_{s,t} 1\{y_{s,t} = y_t\} / \sum_s T_s$, the overall percentage of syllables among all songs. We set each $\alpha_{trans,j}$ at the value for which $p_0(H_{0,trans,j}) = p_0(k_{trans,j} = 1) = 1/2$. For the remaining fixed hyper-parameters, we set $a_{trans,0} = a_{trans,1} = b_{trans,0} = b_{trans,1}^{(0)} = 1$. In numerical experiments, results were robust to these choices.

S.1.2 Hyper-Parameters for Inter-Syllable Intervals

For the inference of the inter-syllable intervals, $\alpha_{isi,00}$ is set to 1 and the global probability vector $\lambda_{isi,00}(\cdot)$ is the ratio of the component size, determined via k -means, over the total sample size. Similar to the syllable transitions, we set $a_{isi,0} = a_{isi,1} = b_{isi,0} = b_{isi,1}^{(0)} = 1$, and, as before, the results were seen to be robust to these choices.

Now we discuss how we determine the number of mixture components, K . To find a suitable choice for K , one use the log pseudo marginal likelihood (LPML) (Geisser and Eddy, 1979) or the widely applicable information criterion (WAIC) (Watanabe, 2010), which are easily calculated and hence particularly useful for complex Bayesian hierarchical models like ours. Specifically, let $f(\tilde{\tau}_{s,t} | \alpha, \beta, \pi)$ be the mixture gamma density function for the transformed ISI $\tilde{\tau}_{s,t}$ with shape and rate parameters α, β and mixture probabilities π . The LPML and the WAIC are then defined as follows.

$$LPML = - \sum_{s,t} \log \left[\mathbb{E}_{\alpha, \beta, \pi | \tilde{\tau}} \left\{ \frac{1}{f(\tilde{\tau}_{s,t} | \alpha, \beta, \pi)} \right\} \right],$$

$$WAIC = -2 \left[\sum_{s,t} \log \mathbb{E}_{\alpha, \beta, \pi | \tilde{\tau}} \{f(\tilde{\tau}_{s,t} | \alpha, \beta, \pi)\} - p_{WAIC} \right],$$

where $p_{WAIC} = 2 \sum_{s,t} \left[\log \mathbb{E}_{\alpha, \beta, \pi | \tilde{\tau}} \{f(\tilde{\tau}_{s,t} | \alpha, \beta, \pi)\} - \mathbb{E}_{\alpha, \beta, \pi | \tilde{\tau}} \{\log f(\tilde{\tau}_{s,t} | \alpha, \beta, \pi)\} \right]$.

They can be straightforwardly estimated using the MCMC samples of α, β, π .

Figure S.1 displays the LPML (left) and WAIC (right) for mixture gamma distributions with $K \in \{2, 3, 4, 5, 6, 8, 10\}$ mixture components. Larger values of LPML and smaller values of WAIC indicate better model fits. We see that $K = 2$ and $K = 3$ have much worse scores compared to $K \geq 4$, suggesting that three or fewer components are highly insufficient. Starting at $K = 4$, both the LPML and WAIC scores converge, suggesting that having more than four components does not improve the fit significantly. By Occam's razor principle, among the models with similar fit, we choose the simplest one, that is, $K = 4$.

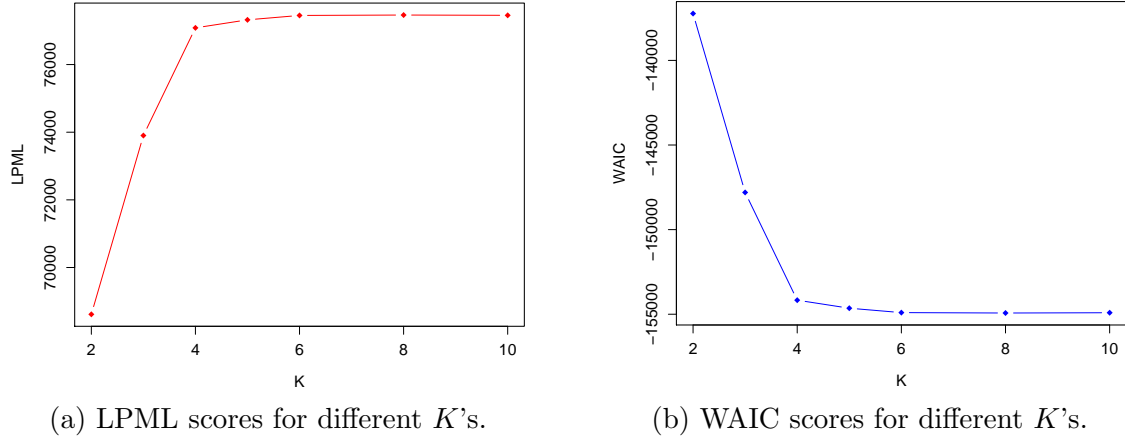


Figure S.1: Results of the model comparison for $K = 2, 3, 4, 5, 6, 8, 10$, including LPML (left) and WAIC (right) scores. Larger values of LPML and smaller values of WAIC indicate better model fits.

S.2 MCMC Initialization

S.2.1 Initialization for Syllable Transitions

For the two covariates, genotype and social contexts, we initialize $\boldsymbol{\mu}_{trans,1} = (1/2, 1/2)^T$ and $\boldsymbol{\mu}_{trans,2} = (1/3, 1/3, 1/3)^T$. We assume, at the beginning of the simulation, that each covariate value has its own cluster and initialize $z_{trans,j,h}$ at h for $h = 1, \dots, d_j$. Accordingly, the associated $\boldsymbol{\lambda}_{trans,h_1,h_2}(y_t \mid y_{t-1})$ are initialized at $\sum_{s,t} 1\{y_{s,t} = y_t, y_{s,t-1} = y_{t-1}, x_{s,1} = h_1, x_{s,2} = h_2\} / \sum_{s,t} 1\{y_{s,t-1} = y_{t-1}, x_{s,1} = h_1, x_{s,2} = h_2\}$. The individual effect $\boldsymbol{\lambda}^{(i)}(y_t \mid y_{t-1})$ is initialized at $\sum_{s,t} 1\{y_{s,t} = y_t, y_{s,t-1} = y_{t-1}, i_s = i\} / \sum_{s,t} 1\{y_{s,t-1} = y_{t-1}, i_s = i\}$. For each y_{t-1} and i , $\{\pi_{trans,0}^{(i)}(y_{t-1}), \pi_{trans,1}^{(i)}(y_{t-1})\}$ is initialized at $(0.8, 0.2)$, indicating a higher initial probability for population-level effect.

S.2.2 Initialization for Inter-Syllable Intervals

For the gamma mixtures, we use k -means to form the initial $K = 4$ components and set $z_{isi,s,t}$ as the label of the component based on the results of k -means. Similar to syllable transitions, we initialize $\{\pi_{isi,0}^{(i)}(k), \pi_{isi,1}^{(i)}(k)\}$ as $(0.8, 0.2)$ for each i and $k = 1, \dots, K$. We assume, initially, that each level of x_r for covariate r forms its own clusters and initialize the latent cluster allocation variables $z_{isi,r,w}$ at w for $w = 1, \dots, d_r$ for $r = 1, 2, 3$. Then the population-level mixture probability vector is set to $\boldsymbol{\lambda}_{isi,g_1,g_2,g_3}(k) = \sum_{s,t} 1\{z_{isi,s,t} = k, x_{s,1} = g_1, x_{s,2} = g_2, y_{s,t-1} = g_3\} / \sum_{s,t} 1\{x_{s,1} = g_1, x_{s,2} = g_2, y_{s,t-1} = g_3\}$ for $k = 1, \dots, K$. The individual-level mixture probability vector $\boldsymbol{\lambda}_{isi}^{(i)}(k)$ is initialized at $\sum_{s,t} 1\{z_{isi,s,t} = k, i_s = i\} / \sum_{s,t} 1\{i_s = i\}$ for $k =$

$1, \dots, K$. The mean probability vector $\boldsymbol{\lambda}_{isi,0}$ is initialized at $\boldsymbol{\lambda}_{isi,00}$.

S.3 Posterior Computation

Samples are drawn from the posterior using a Gibbs sampler that exploits the conditional independence relationships depicted in (2) and (5) in the main paper. For convenience, we use a generic variable ζ to denote all other variables, including data points. In the following two sub-sections, we detail the step-by-step posterior computation for each variable of the syllable transitions and ISIs, respectively.

S.3.1 Posterior Computation for Syllable Transitions

1. Sample each $z_{trans,j,\ell}$ according to its multinomial full conditional

$$p(z_{trans,j,\ell} = h_j \mid z_{trans,j',\ell} = h_{j'}, j' \neq j, \zeta) \propto \mu_{trans,h_j}^{(j)} \times \prod_{y_{t-1}} \prod_{(h_1, h_2)} \frac{\beta\{\alpha_{trans,0}\lambda_{trans,0}(1 \mid y_{t-1}) + n_{h_1, h_2}(1 \mid y_{t-1}), \dots, \alpha_{trans,0}\lambda_{trans,0}(4 \mid y_{t-1}) + n_{h_1, h_2}(4 \mid y_{t-1})\}}{\beta\{\alpha_{trans,0}\lambda_{trans,0}(1 \mid y_{t-1}), \dots, \alpha_{trans,0}\lambda_{trans,0}(4 \mid y_{t-1})\}},$$

where $n_{h_1, h_2}(y_t \mid y_{t-1}) = \sum_{s,t} 1\{y_{s,t} = y_t, y_{s,t-1} = y_{t-1}, v_{trans,s,t} = 0, z_{trans,1,x_{s,1}} = h_1, z_{trans,2,x_{s,2}} = h_2\}$. Note that $v_{trans,s,t} \in \{0, 1\}$'s are latent variables for $y_{s,t}$'s, indicating if the transition probability follows the population-level effect ($v_{trans,s,t} = 0$) or the individual-level effect ($v_{trans,s,t} = 1$), as in Sarkar *et al.* (2018).

2. Sample each $\boldsymbol{\mu}_{trans,j}$ according to its Dirichlet full conditional

$$\{\mu_{trans,j}(1), \dots, \mu_{trans,j}(d_j)\} \mid \zeta \sim \text{Dir}\{\alpha_{trans,j} + n_j(1), \dots, \alpha_{trans,j} + n_j(d_j)\},$$

where $n_j(h) = \sum_{\ell=1}^{d_j} 1\{z_{trans,j,\ell} = h\}$.

3. Sample each $v_{trans,s,t}$ according to its Bernoulli full conditional

$$p(v_{trans,s,t} = v \mid i_s = i, \zeta) \propto \pi_{trans,v}^{(i)}(y_{s,t-1}) \times \tilde{\lambda}_{trans,v}(y_{s,t} \mid y_{s,t-1}),$$

where $\tilde{\lambda}_{trans,0}(\cdot \mid y_{t-1}) = \boldsymbol{\lambda}_{trans,h_1, h_2}(\cdot \mid y_{t-1})$ with $(z_{trans,1,x_{s,1}}, z_{trans,2,x_{s,2}}) = (h_1, h_2)$, and $\tilde{\lambda}_{trans,1}(\cdot \mid y_{t-1}) = \boldsymbol{\lambda}_{trans}^{(i)}(\cdot \mid y_{t-1})$.

4. Sample $\boldsymbol{\pi}_{trans}^{(i)} = \{\pi_{trans,0}^{(i)}(y_{t-1}), \pi_{trans,1}^{(i)}(y_{t-1})\}^T$'s according to its Beta full conditional

$$\{\pi_{trans,0}^{(i)}(y_{t-1}), \pi_{trans,1}^{(i)}(y_{t-1})\} \mid \zeta \sim \text{Beta}\left\{a_{trans,0} + n_0^{(i)}(y_{t-1}), a_{trans,1} + n_1^{(i)}(y_{t-1})\right\},$$

where $n_v^{(i)}(y_{t-1}) = \sum_{s,t} 1\{v_{trans,s,t} = v, y_{s,t-1} = y_{t-1}, i_s = i\}$.

5. Sample each $\lambda_{trans}^{(i)}(\cdot | y_{t-1})$'s according to its Dirichlet full conditional

$$\{\lambda_{trans}^{(i)}(1 | y_{t-1}), \dots, \lambda_{trans}^{(i)}(4 | y_{t-1})\} | \zeta \sim \text{Dir} \left\{ \alpha_{trans}^{(0)} \lambda_{trans,0}(1 | y_{t-1}) + n^{(i)}(1 | y_{t-1}), \dots, \alpha_{trans}^{(0)} \lambda_{trans,0}(4 | y_{t-1}) + n^{(i)}(4 | y_{t-1}) \right\},$$

where $n^{(i)}(y_t | y_{t-1}) = \sum_{s,t} 1\{y_{s,t} = y_t, y_{s,t-1} = y_{t-1}, v_{trans,s,t} = 1, i_s = i\}$.

6. Sample each $\lambda_{trans,h_1,h_2}(\cdot | y_{t-1})$ according to its Dirichlet full conditional

$$\{\lambda_{trans,h_1,h_2}(1 | y_{t-1}), \dots, \lambda_{trans,h_1,h_2}(4 | y_{t-1})\} | \zeta \sim \text{Dir} \left\{ \alpha_{trans,0} \lambda_{trans,0}(1 | y_{t-1}) + n_{h_1,h_2}(1 | y_{t-1}), \dots, \alpha_{trans,0} \lambda_{trans,0}(4 | y_{t-1}) + n_{h_1,h_2}(4 | y_{t-1}) \right\},$$

where $n_{h_1,h_2}(y_t | y_{t-1}) = \sum_{s,t} 1\{y_{s,t} = y_t, y_{s,t-1} = y_{t-1}, v_{trans,s,t} = 0, z_{trans,1,x_1} = h_1, z_{trans,2,x_2} = h_2\}$.

7. For $\ell = n_{h_1,h_2}(y_t | y_{t-1})$, sample auxiliary variables $v_{\ell,h_1,h_2}(y_t | y_{t-1})$

$$v_{\ell,h_1,h_2}(y_t | y_{t-1}) | \zeta \sim \text{Bernoulli} \left\{ \frac{\alpha_{trans,0} \lambda_{trans,0}(y_t | y_{t-1})}{\ell - 1 + \alpha_{trans,0} \lambda_{trans,0}(y_t | y_{t-1})} \right\}.$$

Set $v_{h_1,h_2}(y_t | y_{t-1}) = \sum_{\ell} v_{\ell,h_1,h_2}(y_t | y_{t-1})$. Likewise, for $\ell = 1, \dots, n^{(i)}(y_t | y_{t-1})$, sample auxiliary variables $v_{\ell}^{(i)}(y_t | y_{t-1})$ as

$$v_{\ell}^{(i)}(y_t | y_{t-1}) | \zeta \sim \text{Bernoulli} \left\{ \frac{\alpha_{trans}^{(0)} \lambda_{trans,0}(y_t | y_{t-1})}{\ell - 1 + \alpha_{trans}^{(0)} \lambda_{trans,0}(y_t | y_{t-1})} \right\}.$$

Set $v^{(i)}(y_t | y_{t-1}) = \sum_{\ell} v_{\ell}^{(i)}(y_t | y_{t-1})$. Additionally, sample auxiliary variables

$$\begin{aligned} r_{h_1,h_2}(y_{t-1}) | \zeta &\sim \text{Beta}\{\alpha_{trans,0} + 1, n_{h_1,h_2}(y_{t-1})\}, \\ s_{h_1,h_2}(y_{t-1}) | \zeta &\sim \text{Bernoulli} \left\{ \frac{n_{h_1,h_2}(y_{t-1})}{n_{h_1,h_2}(y_{t-1}) + \alpha_{trans,0}} \right\}, \\ r^{(i)}(y_{t-1}) | \zeta &\sim \text{Beta}\{\alpha_{trans}^{(0)} + 1, n^{(i)}(y_{t-1})\}, \\ s^{(i)}(y_{t-1}) | \zeta &\sim \text{Bernoulli} \left\{ \frac{n^{(i)}(y_{t-1})}{n^{(i)}(y_{t-1}) + \alpha_{trans}^{(0)}} \right\}, \end{aligned}$$

where $n_{h_1,h_2}(y_{t-1}) = \sum_{y_t} n_{h_1,h_2}(y_t | y_{t-1})$ and $n^{(i)}(y_{t-1}) = \sum_{y_t} n^{(i)}(y_t | y_{t-1})$. Set $v(y_t | y_{t-1}) = \sum_{h_1,h_2} v_{h_1,h_2}(y_t | y_{t-1}) + \sum_i v^{(i)}(y_t | y_{t-1})$. Also, set $v_0 =$

$\sum_{y_t} \sum_{y_{t-1}} \sum_{h_1, h_2} v_{h_1, h_2}(y_t \mid y_{t-1}), v^{(0)} = \sum_{y_t} \sum_{y_{t-1}} \sum_i v^{(i)}(y_t \mid y_{t-1}), \log r_0 = \sum_{y_{t-1}} \sum_{h_1, h_2} \log r_{h_1, h_2}(y_{t-1}), s_0 = \sum_{y_{t-1}} \sum_{h_1, h_2} s_{h_1, h_2}(y_{t-1}), \log r^{(0)} = \sum_{y_{t-1}} \sum_i \log r^{(i)}(y_{t-1}),$ and $s^{(0)} = \sum_{y_{t-1}} \sum_i s^{(i)}(y_{t-1}).$

8. Sample $\alpha_{trans,0}$ and $\alpha_{trans}^{(0)}$ according to their gamma full conditionals

$$\begin{aligned} \alpha_{trans,0} \mid \zeta &\sim \text{Ga}(a_{trans,0} + v_0 - s_0, b_{trans,0} - \log r_0), \\ \alpha_{trans}^{(0)} \mid \zeta &\sim \text{Ga}(a_{trans}^{(0)} + v^{(0)} - s^{(0)}, b_{trans}^{(0)} - \log r^{(0)}). \end{aligned}$$

9. Finally, sample $\lambda_{trans,0}$ according to its Dirichlet full conditional

$$\begin{aligned} \{\lambda_{trans,0}(1 \mid y_{t-1}), \dots, \lambda_{trans,0}(4 \mid y_{t-1})\} \mid \zeta &\sim \\ \text{Dir}\{\alpha_{trans,00} \lambda_{trans,00}(1) + v(1 \mid y_{t-1}), \dots, \alpha_{trans,00} \lambda_{trans,00}(4) + v(4 \mid y_{t-1})\}. \end{aligned}$$

The steps to update the hyper-parameters $\alpha_{trans,0}$, $\alpha_{trans}^{(0)}$ and the global transition distributions $\lambda_{trans,0}$ followed the auxiliary variable sampler in West (1992) and Teh *et al.* (2006).

S.3.2 Posterior Computation for Inter-Syllable Intervals

1. Sample the mixture component latent variable $z_{isi,s,t}$'s

$$\begin{aligned} p(z_{isi,s,t} = k \mid i_s = i, z_{isi,1,x_1} = g_1, z_{isi,2,x_2} = g_2, z_{isi,3,y_{t-1}} = g_3, \zeta) \\ \propto P_{g_1, g_2, g_3}^{(i)}(k) \times \text{Ga}(\tau_{s,t} \mid \alpha_k, \beta_k), \end{aligned}$$

where $P_{g_1, g_2, g_3}^{(i)}(k) = \pi_{isi,0}^{(i)} \lambda_{isi,g_1,g_2,g_3}(k) + \pi_{isi,1}^{(i)} \lambda_{isi}^{(i)}(k)$ for $k = 1, \dots, K$.

2. Similar to transition probabilities, we introduce $v_{isi,s,t}$'s and sample each $v_{isi,s,t}$ according to its Bernoulli full conditional

$$p(v_{isi,s,t} = v \mid i_s = i, \zeta) \propto \pi_{isi,v}^{(i)}(k) \times \tilde{\lambda}_{isi,v}(k),$$

where $\tilde{\lambda}_{isi,0}(\cdot) = \lambda_{isi,g_1,g_2,g_3}(\cdot)$ with $(z_{isi,1,x_1}, z_{isi,2,x_2}, z_{isi,3,y_{t-1}}) = (g_1, g_2, g_3)$, $\tilde{\lambda}_{isi,1}(\cdot) = \lambda_{isi}^{(i)}(\cdot)$.

3. Sample $\pi_{isi}^{(i)} = \{\pi_{isi,0}^{(i)}(y_{t-1}), \pi_{isi,1}^{(i)}(y_{t-1})\}^T$'s according to its Beta full conditional

$$\{\pi_{trans,0}^{(i)}(k), \pi_{trans,1}^{(i)}(k)\} \mid \zeta \sim \text{Beta} \left\{ a_{isi,0} + n_0^{(i)}(k), a_{isi,1} + n_1^{(i)}(k) \right\},$$

where $n_v^{(i)}(k) = \sum_{s,t} 1\{z_{isi,s,t} = k, v_{isi,s,t} = v, i_s = i\}$.

4. Sample each $\lambda_{isi}^{(i)}(\cdot)$'s according to its Dirichlet full conditional

$$\{\lambda_{isi}^{(i)}(1), \dots, \lambda_{isi}^{(i)}(K)\} \mid \zeta \sim \text{Dir} \left\{ \alpha_{isi}^{(0)} \lambda_{isi,0}(1) + n^{(i)}(1), \dots, \alpha_{isi}^{(0)} \lambda_{isi,0}(K) + n^{(i)}(K) \right\},$$

where $n^{(i)}(k) = \sum_{s,t} 1\{z_{isi,s,t} = k, v_{isi,s,t} = 1, i_s = i\}$.

5. Sample each $\lambda_{isi,g_1,g_2,g_3}(\cdot)$ according to its Dirichlet full conditional

$$\begin{aligned} \{\lambda_{isi,g_1,g_2,g_3}(1), \dots, \lambda_{isi,g_1,g_2,g_3}(K)\} \mid \zeta \sim \\ \text{Dir}\{\alpha_{isi,0} \lambda_{isi,0}(1) + n_{g_1,g_2,g_3}(1), \dots, \alpha_{isi,0} \lambda_{isi,0}(K) + n_{g_1,g_2,g_3}(K)\}. \end{aligned}$$

where $n_{g_1,g_2,g_3}(k) = \sum_{s,t} 1\{z_{isi,s,t} = k, v_{isi,s,t} = 0, z_{isi,1,x_1} = g_1, z_{isi,2,x_2} = g_2, z_{isi,3,y_{t-1}} = g_3\}$.

6. Sample hyper-parameters $\alpha_{isi,0}$ and $\alpha_{isi}^{(0)}$ using the approximation method introduced in West (1992) for large sample size

$$\begin{aligned} \alpha_{isi,0} \mid \zeta &\sim \text{Ga}\{a_{isi,0} + K - 1, b_{isi,0} + \gamma + \log(n)\}, \\ \alpha_{isi}^{(0)} \mid \zeta &\sim \text{Ga}\left\{a_{isi}^{(0)} + K - 1, b_{isi}^{(0)} + \gamma + \log(n)\right\}, \end{aligned}$$

where n is the sample size and γ is the Euler's constant.

7. Sample the mean probability vector $\lambda_{isi,0}$ as follows. First, for $\ell = 1, \dots, n_{g_1,g_2,g_3}(k)$, we sample the auxiliary variable ω_ℓ as

$$\omega_\ell \mid \zeta \sim \text{Bernoulli} \left\{ \frac{\alpha_{isi,0} \lambda_{isi,0}(k)}{\ell - 1 + \alpha_{isi,0} \lambda_{isi,0}(k)} \right\}.$$

We set $m_{g_1,g_2,g_3}(k) = \sum_\ell \omega_\ell$, $m_0(k) = \sum_{g_1,g_2,g_3} m_{g_1,g_2,g_3}(k)$. We then sample $\lambda_{isi,0}$ as

$$\lambda_{isi,0} \mid \zeta \sim \text{Dir}\{\alpha_{isi,00}/K + m_0(1), \dots, \alpha_{isi,00}/K + m_0(K)\}.$$

8. Sample the mixture gamma shape and rate parameters α_k 's and β_k 's

As discussed in Section 4 in the main paper, we use an approximation algorithm introduced in Miller (2019) to sample the shape parameters α_k 's. Let $\alpha_k^{(i-1)}$ and $\beta_k^{(i-1)}$ be the shape and rate parameter from MCMC iteration $i - 1$. Initialize the

parameters of the gamma conditional, A_k and B_k , for $\alpha_k^{(i)}$ as follows:

$$\begin{aligned}\mu_k &= \alpha_k^{(i-1)} / \beta_k^{(i-1)}, \\ T_k &= S_k / \mu_k - R_k + n_k \log(\mu_k) - n_k, \\ A_k &= a_{isi,0} + n_k / 2, \\ B_k &= b_{isi,0} + T_k,\end{aligned}$$

where $R_k = \sum_{z_{isi,s,t}=k} \log(\tau_{s,t})$, $S_k = \sum_{z_{isi,s,t}=k} \tau_{s,t}$ and $n_k = 1\{z_{isi,s,t} = k\}$.

Let M be the maximum allowed number of iterations. We iteratively compute A_k and B_k until convergence. For iteration $1, \dots, M$, compute the following:

$$\begin{aligned}a_k &= A_k / B_k, \\ A_k &= a_{isi,0} - n a_k + n a_k^2 \psi'(a_k), \\ B_k &= b_{isi,0} + (A_k - a_{isi,0}) / a_k - n_k \log(a_k) + n_k \psi(a_k) + T_k,\end{aligned}$$

and return A_k and B_k if $|a_k / (A_k / B_k) - 1| < \epsilon$ for some predetermined tolerance ϵ . Note that $\psi(\cdot)$ and $\psi'(\cdot)$ represent the digamma and trigamma function, respectively. Given A_k and B_k , the shape and rate parameter for the current iteration i , $\alpha_k^{(i)}$ and $\beta_k^{(i)}$, can be obtained via their gamma full conditionals

$$\begin{aligned}\alpha_k^{(i)} &\sim \text{Ga}(A_k, B_k), \\ \beta_k^{(i)} &\sim \text{Ga}\left(1 + \alpha_k^{(i)} n_k, 1 + S_k\right).\end{aligned}$$

9. Update the covariate cluster parameters \mathbf{k}_{isi} and $\mathbf{z}_{isi,r}$'s

Recall $\mathbf{k}_{isi} = (k_{isi,1}, k_{isi,2}, k_{isi,3})$ represents the number of clusters for each covariate r and $\mathbf{z}_{isi,r} = (z_{isi,r,1}, \dots, z_{isi,r,d_r})$ indicate the cluster allocation for each level of covariate r . For each covariate r , values of $\mathbf{z}_{isi,r}$ partition d_r levels into $k_{isi,r}$ clusters. The constructed clusters are denoted by $\mathcal{C}_{isi}^{(r)} = \{\mathcal{C}_{isi,g_r}^{(r)}\}_{g_r=1}^{k_{isi,r}}$ for covariate r . If $z_{isi,r,w} = g_r$, the w^{th} level of covariate r belongs to the g_r^{th} cluster in $\mathcal{C}_{isi}^{(r)}$. After integrating out $\boldsymbol{\lambda}_{isi,g_1,g_2,g_3}$ and conditioning on the cluster configurations $\{\mathcal{C}_{isi}^{(r)}\}_{r=1}^3$, we have

$$p(\mathbf{z}_{isi,r} \mid \{\mathcal{C}_{isi}^{(r)}\}, \boldsymbol{\zeta}) = \prod_{g_1, g_2, g_3} \frac{\beta\{\alpha_{isi,0} \lambda_{isi,0}(1) + n_{g_1, g_2, g_3}(1), \dots, \alpha_{isi,0} \lambda_{isi,0}(K) + n_{g_1, g_2, g_3}(K)\}}{\beta\{\alpha_{isi,0} \lambda_{isi,0}(1), \dots, \alpha_{isi,0} \lambda_{isi,0}(K)\}},$$

where $n_{g_1, g_2, g_3}(k) = \sum_{s,t} 1(z_{isi,s,t} = k, z_{isi,1,x_1} = g_1, z_{isi,2,x_2} = g_2, z_{isi,3,y_{t-1}} = g_3)$.

To update the values of \mathbf{k}_{isi} 's, we do the following. If $k_{isi,r} < d_r$, we propose to increase $k_{isi,r}$ by 1 by randomly splitting a cluster into two. If $k_{isi,r} > 1$, we propose

to decrease $k_{isi,r}$ by 1 by randomly merging two clusters. We accept the new clustering if the log likelihood of the proposed move is greater than a sampled value from the log-uniform distribution.

In all our examples, we ran 10,000 MCMC iterations with the first 2,000 as burn-ins. Additionally, the rest of the samples are thinned by an interval of 5. MCMC diagnostic plots show no issues in mixing or convergence. The input of our program is a cleaned data set consisting of 70818 rows and 6 columns: mouse ID, genotype, social context, preceding syllable, current syllable, and ISI length. We refer interested readers to Sarkar *et al.* (2018) for details of the implementation of the model for the syllable transitions. We provide R scripts for inference of the ISIs as part of the Supplemental Materials.

References

Geisser, S. and Eddy, W. F. (1979). A predictive approach to model selection. *Journal of the American Statistical Association*, **74**, 153–160.

Miller, J. W. (2019). Fast and accurate approximation of the full conditional for gamma shape parameters. *Journal of Computational and Graphical Statistics*, **28**, 476-480.

Sarkar, A., Chabout, J., Macopson, J. J., Jarvis, E. D., and Dunson, D. B. (2018). Bayesian semiparametric mixed effects Markov models with application to vocalization syntax. *Journal of the American Statistical Association*, **113**, 1515-1527.

Teh, Y. W., Jordan, M. I., Beal, M. J., and Blei, D. M. (2006). Hierarchical Dirichlet processes. *Journal of the American Statistical Association*, **101**, 1566-1581.

Watanabe, S. (2010). Asymptotic equivalence of Bayes cross validation and widely applicable information criterion in singular learning theory. *Journal of Machine Learning Research*, **11**, 3571–3594.

West, M. (1992). Hyperparameter estimation in Dirichlet process mixture models. Institute of Statistics and Decision Sciences, Duke University, Durham, USA, Technical report.